Pile setup in sand – the "PAGE" joint industry project

David Cathie [i], Richard Jardine [ii], Rui Silvano [i], Stavroula Kontoe [ii] and Felix Schroeder [iii]

i) Cathie Group, Belgium.

ii) Department of Civil and Environmental Engineering, Imperial College London, UK.

iii) Geotechnical Consulting Group LLP, London, UK.

ABSTRACT

The reliability of long-term axial capacity predictions for large, offshore-scale, piles is uncertain. Current databases of static load tests include very few entries with diameters ≥ 1m, and none >2m. Also, most of the available tests were conducted at relatively early ages after driving. The PAGE Joint Industry Project addressed this knowledge gap by collating and analysing dynamic driving data from 25 offshore piles with 1.6 to 3.4m outside diameters and contrasting these with dynamic re-strike tests conducted between 1h and 1 year after driving. Systematic signal matching was performed with two independent codes that applied different soil models and the outcomes were compared with predictions from modern CPT-based static capacity design methods. Additional supporting analyses were performed on other piles, where static and dynamic tests had been conducted, to help assess the relationships between statically and dynamically measured resistances. Piles with 0.3 to 3.5m outside diameters followed broadly common trends over the first 30 days after driving, with shaft capacities approximately doubling. While smaller (<1m) diameter piles driven at onshore/nearshore sites display marked further capacity growth, larger offshore piles showed little additional capacity gain after 30 days. The CPT-based Unified offshore pile design method offered conservative predictions for long-term shaft resistance, while no bias was apparent with the ICP-05 approach. An inverse relationship was identified between long-term shaft setup and diameter, which is ascribed to enhanced dilatancy applying at the pile-sand interface. The base capacities interpreted from dynamic analyses consistently fell far below the monotonic loading capacities predicted by current design methods and showed no significant trend to increase over time.

Keywords: driven piles, sand, axial capacity, time effects, influence of scale

1 INTRODUCTION

1.1 PAGE project background

The question of how axial capacity varies with time for piles driven in sands has yet to reach any widely agreed consensus; Jardine et al (2006), Karlsrud et al (2014) or Gavin et al (2015). The main difficulty for offshore, port and bridge designers has been the lack of large-scale static testing and therefore uncertainty on how to extrapolate trends established with relatively small piles onshore. This information gap led to the Authors proposing and leading the Pile Ageing (PAGE) Joint Industry Project (JIP).

PAGE aimed to assemble a pan-Industry database of high-quality dynamic testing records, covering a statistically significant number of large-diameter piles, made from typical steels and driven offshore by standard procedures at well-characterised sites with representative ground temperatures and salinity. Applying consistent and rigorous analysis procedures would establish how ageing affects offshore piles in sand. The outcomes would lead to clearer guidance for international offshore practice and design, including calibration against existing axial design methodologies.

This keynote describes the JIP's work and key outcomes. PAGE attracted the support of eight industrial sponsors and six international expert advisers who are gratefully acknowledged at the end of the paper. The project kicked-off on 21st November 2019 and, despite the Covid pandemic, completed in late 2021.

1.2 Project objectives

The main project objectives were:

- Collating a minimum of 25 offshore, large diameter, pile datasets for which high quality site investigation,

driving and restrike records were available.

- Interpreting for each case ground conditions and soil parameters for pile capacity assessment, as well as pile geometry, hammers, blow counts and time-records.
- Identifying other datasets involving smaller onshore and offshore piles (with diameters from 0.45 to 2m) to provide supplementary insights. This included three cases where parallel dynamic and static tests were conducted on comparable piles.
- Careful quality assurance, combined with a systematic, consistent, approach to dynamic data analysis and independent checking of multiple case histories.

Dynamic test interpretation is inherently more subjective and open to more variable outcomes than static pile testing. It was therefore essential to reduce the potential spread of results by applying a standard, physically based, approach in all dynamic stress wave interpretations.

1.3 Earlier studies of setup in sands

Field evidence of marked setup taking place around piles driven in sands was identified in the late 1990s through experiments conducted at a dense sand nearshore test site at Port Ouest, Dunkirk, northern France. As reported by Jardine et al. (2006), seven 457 mm OD, steel tubular piles were driven in association with the GOPAL joint industry project described by Parker et al. (1999). CPTu tests were carried out close to the test piles, adding to earlier intensive stress path laboratory testing at Imperial College along with in-situ profiling, as described by Chow (1997), Kuwano (1999) and Jardine (2013).

Staged first-time, maintained-load, tension load tests to failure on three identical ≈19 m long piles provided the clear evidence presented in Figure 1 of strong growth in shaft resistance over 235 days, without any change in initial axial stiffness. Re-tests on individual piles gave confused and staggered trends that failed to demonstrate the same impressive capacity gains.

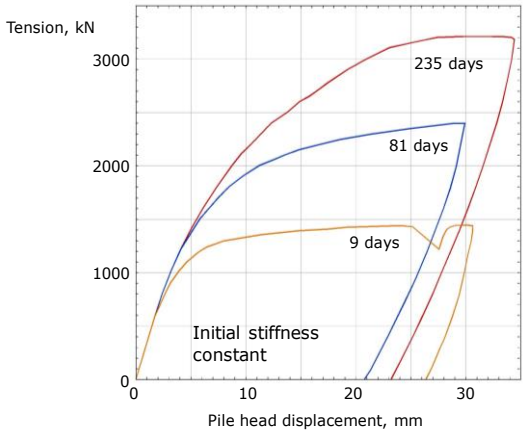

Fig. 1: First-time static tests on identical piles driven at Dunkirk, after Jardine et al (2006).

Adding data from a longer-term test by Chow (1997) on a 324 mm OD, 21 m long, tubular steel pile driven earlier nearby by the CLAROM (Conseil de Liaison des Associations de Recherche sur les Ouvrages en Mer) group led Jardine et al. (2006) to conclude the following:

(a) End of driving (EoID) shaft resistances fell ≈30% below the ICP-05 (Jardine et al, 2005) medium-term shaft capacity estimates;

(b) Tension capacities grew to match the ICP estimates around 10 days after driving;

(c) Shaft capacities stabilised around 1 year after driving at values ≈2.4 times the ICP-05 estimates;

(d) Static testing to failure disrupted and set back the beneficial ageing processes;

(e) Cyclic loading could either degrade or enhance capacity growth, depending on the levels applied.

Comparable, but fully independent, 'first-time tension test' programmes were run with tubular piles of similar sizes in dense sand driven above the water table at Blessington, Ireland (Gavin et al., 2013) and in loose, submerged sand at Larvik, Norway (Karlsrud et al., 2014). Their trends were brought together by Rimoy et al. (2015) and Gavin et al. (2015) in Figure 2, where ICP-05 sand shaft capacity predictions are employed to normalise for each site's specific ground profile and identify a common overall ageing trend. The beneficial ageing trends may help to explain why offshore foundation failure has been rare in service, despite the unsatisfactory predictive reliability statistics reported for the Main Text API and ISO procedures reported by Jardine et al (2005), Lehane et al (2017) or Yang et al (2017).

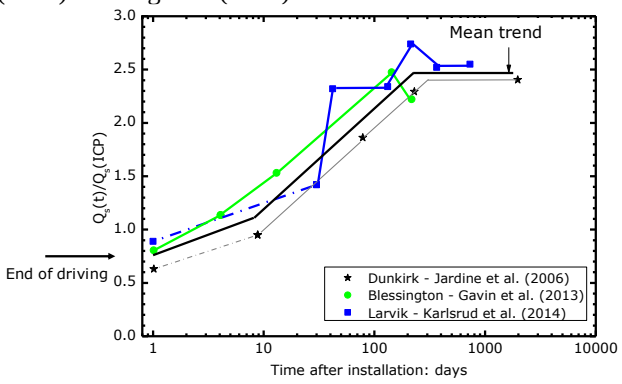

Fig. 2: Trends for growth in first-time shaft capacity with time at three sites, tension capacities normalised by pile specific ICP-05 predictions; after Rimoy et al. (2015).

Jardine et al. (2006) outlined four potential mechanisms that might contribute to the pile ageing processes:

- Physio-chemical and corrosion reactions involving the pile shaft, sand and groundwater leading to higher stationary radial stresses over time;
- Higher interface shearing resistance angles applying after ageing in-situ than are seen in tests employing fresh sands and interfaces;
- Enhanced dilation at the interface boosting radial effective stresses during loading to failure due to either additional radial dilation δr or increased sand stiffness G, or
- Shaft radial stresses rising above those expected by, for example ICP-05, due to stress redistribution linked to creep within the surrounding sand mass.

Chow (1997), Axelsson (2000), Rimoy (2013) and

others report that concrete piles also setup after driving in the field, so it appeared unlikely that the ageing trends of industrial piles were related purely to chemical reactions involving their shaft surfaces. In the same way the pile loading tests shown in Figure 1 indicated that sand stiffness changes were unlikely to be the main driving factor.

Rimoy et al (2015) describe intensive research testing conducted with CPT-scale, highly instrumented, stainless-steel model 'mini-ICP' piles installed in a large, pressurised calibration chamber that explored the potential contributions of the purely mechanical mechanisms to the shaft capacity gains seen in the field. Multiple experiments showed no increase over time in either the stationary shaft radial effective stresses or the dilative radial stress changes invoked by loading to failure.

Addressing the paradox between the field and model piles' ageing trends, Rimoy et al. (2015) suggested that absolute pile diameter may affect the ageing mechanism. The thicknesses of the crusts of crushed sand are found adhering to the mini-pile shafts in the Yang et al. (2010) laboratory tests and in field-driven piles at Dunkirk by Chow (1997), at Blessington (Gavin et al., 2013) and at Eemshaven (where cemented iron hydroxides were identified by Kolk et al. (2005) around the EURIPIDES piles) grew with grain size and relative penetration depth, h, but did not scale up in proportion to pile diameter.

Yang et al. (2010), Rimoy (2013) and Silva (2014) noted the annular thickness of the crushed sand zones represents a far greater proportion of the mini-piles' outside pile diameters than with larger industrial piles. Yang et al. (2010) showed that large compressive volume strains occur within the annular crushed sand zone whose impact on any stress re-distribution mechanism would therefore be far more significant with small-diameter piles. The grain crushing and soil–pile stress redistribution processes are also likely to be affected by the open- or closed-ended, conical or flat, pile tip geometry.

In a similar way, approaches such as the ICP-05 design method predict that (with all other factors held constant) any contribution to capacity generated by enhanced interface dilation would be likely to reduce with increasing pile outside diameter.

Seeking to investigate whether large offshore piles gain shaft capacity over time in sands, Jardine et al. (2015) reviewed data from dynamic stress-wave matching of accelerometer and strain gauge signals recorded during pile driving in very dense marine sands for the Borkum Riffgrund I offshore jacket, which stands in 24 m of water in the German North Sea. Signal matching undertaken for the project with CAPWAP varied the soil resistance profiles until a good match was achieved between the predicted and measured strain and acceleration traces. Analyses of a restrike test on one of the platform's eight (2.13 m OD, 38.5 m penetration) piles indicated indicated 45% shaft capacity growth over the first 6 days after driving that would be hard to assign, under the anoxic conditions applying tens of metres below the North Sea floor, to corrosion reactions. While the shaft resistances showed values greater than expected by the ICP-05 approach, the dynamically measured base resistances fell well below those expected by the ICP-05, or any other common predictive approach. Byrne et al. (2012) report similar findings; it appears that the displacements developed during dynamic hammer blows fall far below those required to mobilise full bearing failure.

Further joint work summarized by Carroll et al (2020) explored the potential influence of corrosion in-situ on piles driven at the three sites considered in Figure 2. Dozens of (50 to 60 mm OD, approximately 2 m long) mild steel and stainless/galvanised steel micro-piles were tested in tension up to 2 years after driving. The micro-piles' ageing was dominated by corrosion reactions that both roughened the shafts and pushed the eventual shaft failure mechanism out into the sand mass. As with the larger piles in Figure 2, the micro-piles' set-up reached stable upper limits within a year. However, stainless steel piles showed no ageing gains and corrodible mild steel micro-piles showed less marked set-up, at the same sites, than the larger piles tested at the same sites. Carroll et al. (2020) concluded that:

- Physio-chemical reactions contribute significantly to the setup of small steel piles driven in sand;
- Other processes contribute to larger concrete and steel industrial driven piles' field setup tends;
- The ageing behaviour of offshore piles may dependent on outside diameter, wall thickness ratio and subsea environmental conditions;
- Installation process also affect ageing. Easily driven piles show higher capacities than those that require hard driving and bored piles do not setup in the same way.

The research reviewed above identified substantial and important capacity growth over time. However, the benefits of setup may depend on pile installation procedure, diameter, wall thickness ratio and potential corrosion reactions controlled by pile steel grade, groundwater salinity, temperature and dissolved oxygen concentrations.

1.4 Further case histories reviewed for PAGE

The PAGE team identified six additional case histories in which dynamic and static measurements have been reported that provide further evidence of field setup trends. As summarised below, all concerned open-ended tubular steel pipe piles with outside diameters exceeding 0.3m driven in (predominantly medium dense to dense) sands.

Südkai project, Hamburg harbour, Germany

Skov and Denver, (1988) report static and dynamic measurements on 0.762m OD (12.7mm wall thickness) pipe piles driven to 33.7m depth with external T-shaped wings over their lower 3m. The ground profile consisted of alternating layers of fine, medium and coarse sand, locally with fine gravel; no indication was given of relative density. Dynamic data was recorded during driving and in a 30 day restrike, with an intermediate static test after 7 days. The axial capacity results and setup are summarised in Table 1. Note that the 30-day re-strike developed a lower (0.8mm) set than is usually required to establish axial capacity and that the pile's long-term setup was probably affected negatively by the intermediate 7 day test.

Table 1: Summary of total axial resistance results Südkai, Hamburg harbour.

Age (days)	Dynamic (CAPWAP) (MN)	Static (MN)	Setup factor (-)
EoID	3.63		
7		4.85 – 5.08(1)	1.34 – 1.40
30	5.17		1.42

(1) Depending on interpretation method

Japanese Association for Steel Pipe Piles (JASPP) tests

Shibata et al (2000) report tests by JASPP on 0.4m OD, 12mm thick pipe piles in which piles were driven and tested in fine and coarse sands characterised by CPT and SPT profiling. After instrumented monitoring during driving, two piles were tested statically and/or statnamically, while one was monitored during multiple restrikes employing different hammer energies. Given the multiple tests conducted on individual piles, the setup factors defined relative to EoID of 1.12, 1.36 and 1.53 after 6, 30 and 52 days respectively, provide lower-bound estimates to the setup of previously unfailed 'virgin' piles.

Dunkirk, Northern France

Chow et al. (1998) reported static tension retests performed at the Dunkirk test site on open-ended piles driven in dense to very dense marine sand. The piles had been driven and tested in 1989 by the French CLAROM research group. CPT cone resistance profiles typically fell between 10 and 20 MPa and identified a band of sand with a significant amount of organic matter at 7-8m. The two piles selected for testing had an outer diameter of 0.324m OD and were driven to depths of 11m and 22m respectively. An 85% increase in shaft capacity was observed between six months and five years after pile driving.

As noted earlier, first time tension tests were performed later at a nearby location on 0.457m OD (13-20mm wall thickness) piles driven to approximately 19m, giving the results presented in Figure 1. Shaft capacities rose over eight months to more than double those seen in load tests conducted a few days after driving or expected from calculation procedures designed to match short-term capacities. Setup factors derived from shaft resistance compared to the expected EoID shaft resistance were around 1.6, 2.6 and 3.6 for the 9 day, 81 day and 235 day tests respectively. Low level one-way load cycling was found to accelerate the beneficial ageing processes.

Los Angeles Export Terminal (LAXT) Wharf, USA

Bushan (2004) and Bushan/Geofon (1997) summarise extensive dynamic testing for the Los Angeles Export Terminal Wharf. Signal matching for EoID and BoR tests conducted 1 to 139 days after driving on nine 1.37m OD (25mm wall thickness) and three 0.91m OD (16mm wall thickness) open steel pipe piles driven to penetrations of 18 to 26m in primarily dense sands and silts, as identified by sampling and CPT profiling, led to the results summarised in Figure 3. Note only End of Restrike (EoR) resistances (recorded after 63 blows) were available for the 139-day case, which considerably under-represent the capacities available at the Beginning of Restrike.

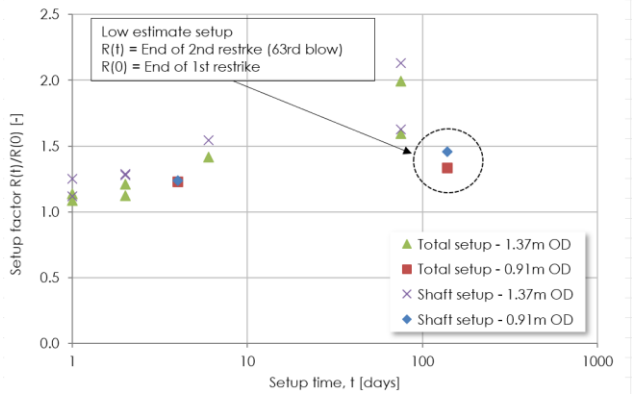

Fig. 3: Setup factor (total resistance and shaft resistance) versus setup time: Los Angeles Export Terminal piles.

Met mast platform pile in German Bight

Kirsch and von Bargen (2012) report EoID and BoR dynamic tests on a 3.35m OD pile driven at a windfarm site dominated by generically dense to very dense sand, with silty sand and also clay layers (around 2m thick) occurring over the mid-section of the pile. Although the precise soil conditions at the test location are not clear, the pile showed a set-up factor of 1.5 after 31 days of ageing.

NGI sand test sites

Karlsrud et al, (2014) summarise 'virgin' static tension tests performed at 1, 2, 6, 12 and 24 month ages on ten tubular driven steel piles at two onshore sites in Norway. The piles driven at their Larvik site had 0.508m OD and penetrated 20.1m into loose to medium dense fine silty sand with some clayey silt layers.

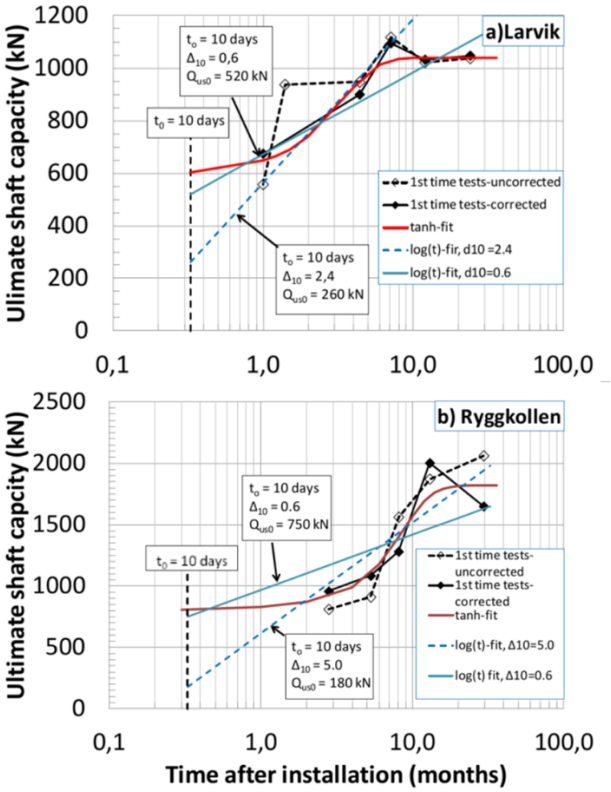

Fig. 4: Tension resistances at NGI test sites, Karlsrud et al, (2014)

Smaller diameter (0.406m OD) piles were driven at their Ryggkollen site to 15.0m through dense medium sand and stony gravel. CPT data were available for Larvik, but not for Ryggkollen. The 1st time shaft resistances observed (and corrected for soil profile variations) are summarised in Figure 4. Rimoy et al (2015) interpreted the data in terms of ICP shaft resistance in tension, adopting an average ICP capacity ≈408 kN. Table 2 presents the results, as re-analysed for PAGE.

Table 2. Normalised uplift shaft resistance from Larvik tests.

Time after installation (days)	Qs(t)/Qs(ICP) (-)
1	0.9
30	1.67
120	2.21
200	2.70
360	2.55
750	2.58

2 PAGE METHODOLOGY

2.1 Approach

The above case histories confirm that shaft capacities increase markedly over time after driving. However, they do not provide convincing evidence of how the shaft and base resistances of large offshore piles vary with time after driving through sands under marine conditions.

The PAGE addressed this lack of knowledge by developing a high-quality database of offshore dynamic test. Critical to this endeavor was developing and applying suitable quality criteria.

2.1 PAGE quality criteria

The ten main quality criteria were:

- Full site investigation data was required close to each pile location, sufficient for application of CPT-based and/or laboratory-based capacity analysis covering the full shaft length and conditions below the pile tip.
- Sand dominated layers should contribute at least 75% of the design total shaft resistance and pile outside diameter should exceed 0.45m.
- The pile dimensions, wall thicknesses, weights, total length and penetrations at EoID and BoR were required, as well as steel grade properties and tolerances.
- The driving configuration, water depth, hammer make and model for EoID and BOR, anvil, helmet and ram masses, connection details and dimensions were required, as were the makeup of any follower, transition piece or cushion.
- The pile driving data should include the contractor's installation procedure and as-installed report, self-weight penetration and a digital driving log.
- The driving hammer energies for initial driving to full penetration and on restrike, as well as the corresponding blow counts (per 250 mm) and set (mm) per blow on restrike. Soil internal plug heights should be known.
- Details of any driving interruptions, driving of nearby piles and add-on lengths were also required, as was information on metocean conditions.
- Dynamic pile testing reports and, where applicable, independent verification report, showing the planned and operational configurations of strain and acceleration sensors. The reports should also identify the penetration depths ranges of the dynamic driving and re-drive signal sets, give the detailed strain and acceleration time history data in text files and assess their quality for at least three consecutive EoID and BOR blows.
- Alternatively, average pile force and velocity time histories could be accepted, provided the processing to achieve these records was detailed fully, including any pre-processing, smoothing, averaging or time-shifting.
- Ageing times between EoID and BoR must be known, as should pile corrosion protection details and whether a CP system operated between EoID and BoR.

It was crucial that the dynamic signal quality was sufficiently high to allow signal matching by the two independent expert teams. The requirements included:

- Strain and acceleration instrument specifications and locations must be known.
- The recorded force/velocity signals, signal lengths and frequencies should show suitable proportionality.
- BoR sets should be sufficient to mobilise the axial resistance. If the sets fell below the limits recommended by PDI (2006) for wave matching, sufficient data had to be available for meaningful alternative 'calibrated wave equation' analyses to be applied.

An overall quality rating was adopted from a weighted average of the sub-ratings. Scoring against these criteria led to closely grouped values in the moderate to high reliability range, for most of the 25 cases accepted by PAGE. The total dataset available from the JIP's pan-industry survey did not offer significant redundancy, especially for cases with extended ageing periods. The checklists and scoring were crucial to deciding whether to accept, or not, any given case, it was not found appropriate to apply the weightings of accepted tests quantitatively in the JIP's analysis.

2.2 Signal matching precepts and overall checking

After carefully assessing input data quality and rigorous checking of how the various dynamic analysis parameters affect the results obtained, standardised approaches were applied for all signal matching analyses. The adopted procedures restricted the shaft and bases SRD profiles to physically reasonable distributions and kept all dynamic parameters within published recommended limits. To address model uncertainty one team employed the well-know CAPWAP (PDI, 2006) package, while the other adopted the research orientated code IMPACT (Randolph, 2008). Setup ratios were established for each offshore case by comparing EoID and BoR resistances.

Comparisons were also made with internationally recognised CPT-based pile resistance calculations to assess their applicability to large diameter offshore piles. Further checking was performed by undertaking 'PAGE

methodology' analyses of high-quality case histories where both static and dynamic testing was conducted at known ages after driving at well-characterised sites.

2.3 Geotechnical data interpretation and axial resistance assessment

Geotechnical

Site characterization began with Robertson (2016) CPT-based soil type classification, with attention to transitional materials to avoid misidentification which may be very significant with CPT-based axial capacity methods. All CPT profiles were manually inspected and adjusted where necessary, including for localised high tip resistance, before engineering calculations were performed. Once the corrected profiles were developed, average tip and sleeve resistance values were assigned every 0.5m from computed running averages evaluated over a window of +/- 0.5m from the CPT depth. Representative q_t values for base resistance calculation were selected according to the requirements of the specific pile capacity method. In the absence of defined criteria, base resistances were found from simple averaging of the smoothed CPT data on a 0.5m grid over depth ranges of 1.5 outside pile diameters above and below the pile tip when conditions were relatively uniform.

In keeping with the individual methods' recommendations, operational interface shear angles δ_{cv} were taken as 29° in sands, unless site-specific interface ring shear measurements were available.

Static pile resistance

Static pile capacity estimates were made with the full ICP-05 (Jardine et al 2005), full UWA-05 (Lehane et al 2005) and the full Unified CPT-based methods were applied. The latter give the best available matches to high-quality databases of static pile load tests; Yang et al (2017), Lehane et al (2017) and (Lehane et al 2020). API main text sand calculations were also considered.

Where any limited clay layers were encountered, their contributions to shaft resistance were assessed where possible by the UWA-13 (Lehane et al 2013) CPT based clay method. Given that the clay layers should comprise no more than 25% of the overall axial capacity, the final outcomes are relatively insensitive to the method chosen. The UWA-13 approach has the advantages of simplicity and incorporating an h/R* term. The ICP-05 or API main text clay calculations were also considered in cases where the UWA-13 CPT method proved difficult to apply.

Soil resistance during driving (SRD)

The method adopted for initial SRD estimation was the Alm and Hamre (2001) approach. The modification proposed by Maynard et al (2019) for large diameter monopiles was not required for the PAGE piles.

2.4 Standardised CAPWAP procedure

A standard procedure was developed for PAGE based on the approach recommended by Pile-Dynamics (2006, 2014), but with a further constraint that the shaft friction distribution should be physically credible considering the soil and CPT-based pile resistance profiles. The two main stages of the procedure were:

- Data quality assessment and preliminary adjustment, followed by signal selection and further adjustment, all in PDA-S system
- Signal matching and static resistance assessment with CAPWAP

The raw data was processed in PDI PDA-S to confirm wave speed, pile geometry inputs, sensor inputs, signal stability, and that pile stresses were below yield, force and velocity signals return to zero and were proportional before first reflections, pile set was reasonable, and that prior and subsequent blows had similar characteristics.

The target pile set was established using the average set/blow (for EoID) or initial blows recorded on restrike (BoR). Blows selected ideally considered a set of 5 – 10mm with average hammer energy. Blows with a set less than 2.5mm were not analysed, except in exceptional cases, to avoid underestimation of the pile resistance. In general, at least 2 blows were analysed for each dataset although other blows were also reviewed to confirm the pile resistance. Acceleration correction factors were introduced to ensure that the final pile top velocity was zero and the velocity integration leads to the pile set.

The signal matching of selected signals then progressed in CAPWAP using primarily the upwardly propagating force wave (wave up). The procedure involved:

- An initial shaft friction distribution from the Alm and Hamre method which was adjusted iteratively from mudline to pile toe to reproduce the measured wave up (i.e. up to 2L/c) maintaining a physically reasonable shaft resistance distribution considering the initial resistance at toe, and friction changes along the shaft. Consistency of distribution between shaft resistance from blows at EOID and BOR was maintained if reasonably possible.
- The unit end bearing being adjusted to reproduce the measured wave up (slightly later than 2L/c), simultaneously adjusting toe quake and toe damping
- Iteration between these two stages until the best match was found for the shaft and end bearing resistances, while maintaining physically reasonable assumptions. When signal matching with radiation damping was performed, adjustments in resistance were accompanied by adjustments in the radiation damping factors.
- When the best match for resistances had been achieved, the analysis proceeded to adjust the quakes and unloading parameters to improve the match.
- The sequence was repeated iteratively ensuring also that the computed and measured sets were consistent.

2.5 Independent approach using IMPACT

Alternative codes offer different soil models to CAPWAP. To obtain the most robust results possible, 12 cases were analysed independently with IMPACT (Randolph, 2008), which employs the Randolph and Simons (1986) shaft resistance model and the Deeks and Randolph (1995) base model. The initial small strain shear modulus profile (Gmax) was derived from correlations with

CPT resistance for each location before iterative adjustment to find a lower operational shear modulus G for each layer. Initial distributions of shaft resistance and end bearing adopted the same approach as in CAPWAP (Alm and Hamre method) and were adjusted during signal matching.

One area of difference is that in IMPACT the soil plug is modelled, and the inside and outside shaft capacity split may be addressed, providing insight into the effect of the different 1D soil plug modelling assumptions. Differences in interface and radiation damping between CAPWAP and IMPACT also affect the results. These differences were examined and discussed within the project team to inform the final standardised CAPWAP signal matching approach which was then adopted for all PAGE signals.

The internal unit shaft resistance is expected to be lower than the external. The internal resistance is controlled by the internal radial stresses, which can relax in the plug as they experience dynamic shaking under constant radial strain conditions constrained by the pile wall. The radial stresses generated by installation are generally larger over the piles' external shaft lengths and have distributions that decay out to the far-field in-situ stress-controlled boundary conditions. In contrast with the internal plug conditions, the stress waves generated by driving are free to radiate out into the surrounding ground.

Theoretically, annular end bearing provides the only source of tip resistance with coring piles, but it is accepted that signal matching may not be able to resolve the high local internal and external skin friction developed near the pile toe from the annular end bearing component. Lumping these components together may lead to overestimating the true annular end bearing. Therefore, the PAGE procedure was to allow the annulus end bearing to be defined by the signal matching. However, any excessively high base bearing results were limited in subsequent iterations if considered unrealistic. Limits to the undrained or near undrained resistance around the pile tip could arise from effects such as pore water cavitation.

In order to standardise the signal matching, the same initial shaft resistance and end bearing were used by the CAPWAP and IMPACT modelling teams. The subsequent signal matching processes led to potentially different final shaft resistance/end bearing distribution that reflect the different modelling assumptions implicit in CAPWAP and IMPACT as well as potential operator-dependency.

2.6 Signal matching - comparison of CAPWAP and IMPACT results

Preliminary exploratory parallel CAPWAP and IMPACT analyses on 8 data sets were performed to select the best approach for the final PAGE signal matching. The parameter cases considered were identified as 1A, 1B, 2A, 2B where 1 refers to the initial Alm and Hamre (2001) distributions, while 2 signifies the adoption of another physically reasonable distribution; letter A refers to a CAPWAP analysis without radiation damping, and B with radiation damping. An example of the findings of these comparison analyses is shown in Figure 5.

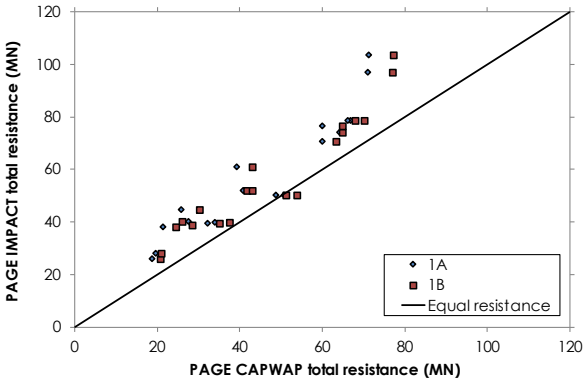

Fig. 5: CAPWAP – IMPACT comparison of total resistance (1A without radiation damping, 1B with radiation damping).

Adopting CAPWAP case 1B (Alm and Hamre initial distribution, with radiation damping) led to the closest agreement with IMPACT as shown in Table 3 and this approach was adopted for all subsequent analyses.

Table 3. IMPACT/CAPWAP resistance ratio (preliminary data set of 8 piles).

	1A	1B	2A	2B
Total resistance	1.33	1.25	1.37	1.27
Total shaft resistance	1.33	1.26	1.36	1.27
Toe resistance	1.36	1.28	1.51	1.37

Considering all datasets finally modelled by both CAPWAP and IMPACT, the results indicate a consistent shaft resistance bias as shown by the example in Figure 6. Note that "total shaft resistance" refers to the single 'shaft resistance' in CAPWAP and the sum of the inside and outside shaft resistances in IMPACT. At later stages of the paper this is referred to simply as 'shaft capacity'.

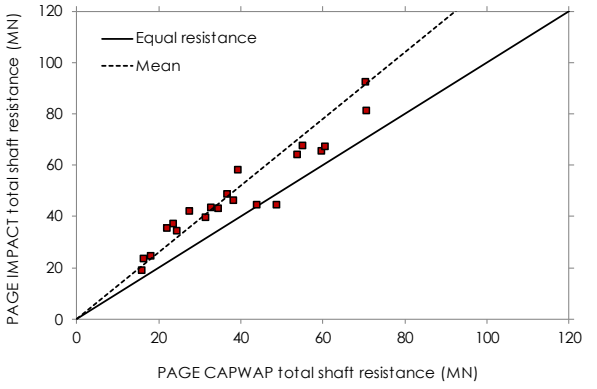

Fig. 6: Comparison of CAPWAP and IMPACT shaft resistance from signal matching.

The average bias between the CAPWAP and IMPACT resistances (RIM/RCW) was 1.28 and 1.30 for total resistance and total shaft resistance, respectively, with coefficients of variation of 0.12 (total) and 0.14 (shaft).

The IMPACT analyses indicate a range between 0.7%-

22.4% for the internal shaft resistance as a portion of the total shaft resistance with a mean of 11.3%. Buckley et al. (2020) adopted a similar approach using IMPACT and showed that the explicit modelling of the soil plug can lead to an improved back analysis of driving records. However, the model adopted for the soil plug in IMPACT is approximate and the precise split between internal and external shaft friction remains uncertain.

The systematic differences in the derived resistance between the two codes (CAPWAP and IMPACT) arises from the different soil response models, as discussed later. Comparisons between static pile test axial resistance and CAPWAP/IMPACT did not lead to any conclusion as to which model was 'better' and were given equal weight. However, when the set was low (< 2.5mm) the IMPACT results were often significantly higher than CAPWAP and gave more plausible indicators of pile resistance. This probably derives from the more rigorous modelling of the energy dissipation into the soil mass in the continuum formulation used in IMPACT.

The systematic differences between the two codes are not apparent when considering setup as shown in Figure 7. This demonstrates that setup is not sensitive to the pile-soil interaction model adopted.

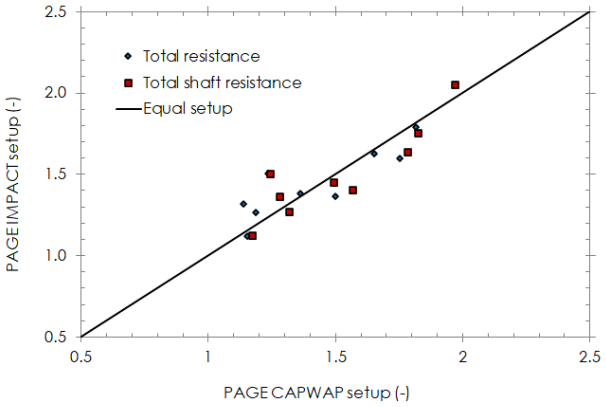

Fig. 7: Comparison of setup factor derived from CAPWAP and IMPACT.

2.7 Calibrated wave equation approach

Eight of the longer term (>50 days) PAGE BoR tests did not achieve the 2.5mm set considered necessary for CAPWAP analyses to indicate the full shaft resistance. Alternative GRLWEAP (PDI, 2010; Rausche et al, 2009) analyses were undertaken for these locations using a calibrated (or refined) wave approach (as well as IMPACT analyses in some cases). Shaft and end bearing resistances were derived from signal matching at EoID using the measured energy (ENTHRU) and observed EoID sets and used to calibrate damping and quake parameters for wave equation analysis. The duly calibrated wave-equation model was then used to estimate the BoR resistance corresponding to the (low) observed set achieved with the hammer employed and so estimate the full resistance that could not be gauged reliably through CAPWAP analyses of the applied blows.

This approach encapsulates the best available practical methodology to identify the conditions at which driving refusal occurs, which is normally defined as sets falling below 1mm per blow. This alternative approach provides a more representative treatment for blows that fail the predefined set criteria, for which signal matching could potentially underestimate piles' static resistances. Unlike signal matching, the calibrated wave equation analyses do not provide additional information on the distribution with depth of shaft resistance.

While signal matching was the preferred approach for all blows that passed the limiting criteria, the alternative treatment was crucial to several of the potentially most valuable long-term offshore re-strike blows.

2.8 Assumptions underpinning signal matching

Signal-matching solutions are not unique and there are multiple solutions which can satisfy the dynamic equilibrium during a blow. The assumption underpinning the signal matching axial resistance assessment is that pile resistance is mobilised fully during the examined blow.

Static load tests, as shown in Figure 1, indicate that the displacements required to reach failure increase as shaft capacities rise through ageing. This could be taken as indicating that higher limiting set values should apply when signal matching re-strikes performed on aged piles. However, the static pile head displacements include the displacements that accumulate from non-linear straining of the surrounding soil mass (integrated out to infinity in principle) under the shear stresses applied over the whole pile surface as well as any local slip near the shaft. In contrast, the set during driving signifies only the final permanent soil-pile slip mobilised locally at the pile-soil interface as the stress wave moves down (and back up) the pile. The large deformations required to reach failure in static tests on aged piles do not necessarily imply that comparable larger sets per blow are required to give reliable re-strike test interpretation.

However, it is important to acknowledge that dynamic measurements inevitably provide less reliable information than static tests and that blows that generate sets that comfortably exceed 2.5mm, and ideally give 5 to 10mm sets, provide more representative information than those with sets below the lower limit.

2.9 Comparison with PDM contractor results

A comparison of the PAGE CAPWAP results, and results obtained by the pile dynamic monitoring (PDM) contractors employed at the time of the installation of the piles are shown in Figure 8 for total resistance. All but one of the contractors employed the CAPWAP software.

This comparison indicates that the PAGE CAPWAP signal matching led to, on average, slightly lower resistances than those obtained by the PDM contractors with average ratios of 1.09 and 1.05 for total resistance and total shaft resistance, respectively. The associated coefficients of variation are 0.18 (total) and 0.24 (shaft). The original PDM contractors' results were not carried further into the PAGE work.

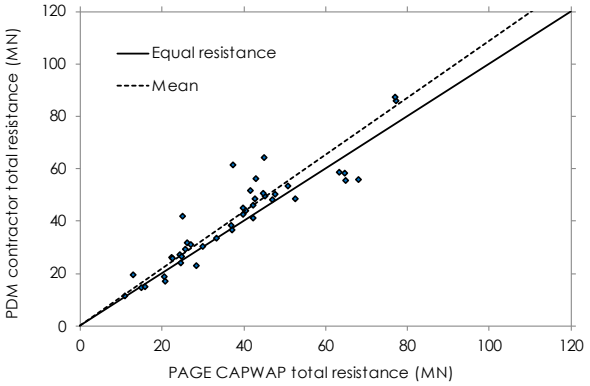

Fig. 8: Comparison of PAGE CAPWAP and PDM contractor total resistance from signal matching

2.10 Model uncertainty

As noted previously signal-matching solutions are not unique; there are multiple solutions which can satisfy the dynamic equilibrium during a blow. This leads to an inherent uncertainty in the signal matching predictions which has been recognised and discussed widely (Fellenius 1988, Svinkin 2004, Buckley et al. 2017).

Buckley et al (2017) explored operator dependency by assigning the same dataset to three independent CAPWAP operators, allowing them to choose the resistance model and associated parameters. The resulting total shaft capacity estimates fell within ±4% of the mean, while the differences in total capacities were more significant within approximately ±10% of the mean value, highlighting the greater uncertainty of base matches. Significant differences were also found in the interpreted mobilised shaft friction profiles despite the good match in terms of total shaft capacities. Furthermore, the operator dependency varied with the relative ease of driving conditions.

The PAGE methodology aimed at limiting the operator dependency by standardising the process by adopting consistent initial profiles, input signals and 'reality' checks for the results between multiple adjacent blows, while recognising that operator dependency cannot be eliminated. The choice of soil resistance model is probably the major source of epistemic uncertainty as clearly seen in the predictions for cases 2A and 2B (Table 3) conducted by the same CAPWAP operator. These indicate differences of 7% and 10% for the total shaft and toe resistances respectively.

The CAPWAP and IMPACT axial resistances showed consistent variations which are attributed principally to their different soil resistance models, as discussed below. The comparison also highlighted the higher uncertainty in the base predictions which is due to: i) potential residual axial stresses generated after each blow which are not explicitly simulated; ii) insufficient displacements to mobilise the pile's end bearing capacity during driving or restrike (Randolph, 2003; Salgado et al., 2015); iii) difficulty of resolving wave reflections arising from the pile annulus and the pile shaft very close to the toe. However, setup factors calculated as EoD/BoR ratios showed less divergence between the independent analyses.

2.10 CAPWAP and IMPACT soil models

The reliability of signal matching is directly connected to how well the pile-soil model captures the actual behaviour of the pile-soil system. The mechanical concepts of the alternative pile-soil models are presented in Figure 9.

The soil models used in CAPWAP and GRLWEAP are based on the rheological model developed by Smith (1960), with the soil shaft resistance expressed as (for the "Smith viscous" model):

$$\tau = Min\left(1, \frac{w_p}{Q_{s_{quake}}}\right)\left(1 + J_s v_p\right)\tau_s \qquad (2)$$

Where:

τ = Dynamic and limiting static shaft resistance
τ_s = Limiting static shaft resistance
w_p = Local pile displacement
v_p = Local pile velocity
Q_{s_quake} = The 'quake' parameter, representing the displacement for which the limiting static resistance is fully mobilised
J_s = Smith's damping parameter

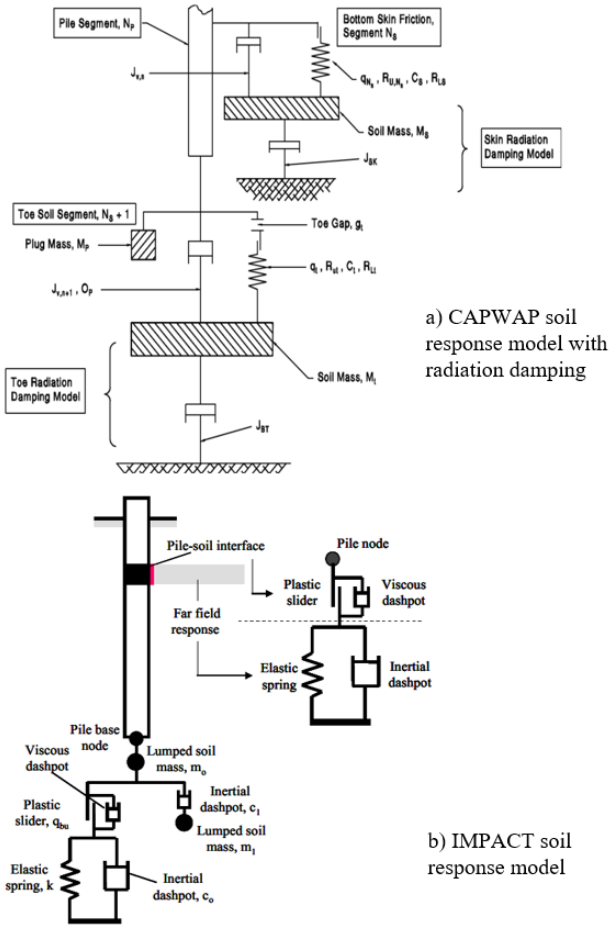

Fig. 9: Soil response models in CAPWAP and IMPACT, (a) PDI, 2006; b) Randolph, 2008.

The application of the Smith model at a pile shaft node cannot differentiate between viscous and inertial damping

during driving. Additionally, the soil resistance on the internal pile walls of open-ended piles is not distinguished from their outer soil resistance. Smith's base model adopts a similar formula to Equation (2)

With regards to model parameters, Rausche et al (2010) gave typical value of the shaft quake, Q_(s_quake), ranging from 1.0 – 7.5 mm for sands and clays, and the toe quake, Q_(b_quake), in the range of 1.0 mm to maximum pile toe displacement. An extension to the Smith soil model was introduced by adding soil mass to incorporate the effects of radiation damping – energy that is dissipated into the soil mass due to inertial and stiffness effects of the soil outside the pile-soil interface as shown in Figure 9a.

IMPACT applies a more sophisticated soil resistance model (referred to as the 'continuum model') based on the closed-form solution of Novak et al. (1978); see Simons and Randolph (1985) and Randolph (2003). Figure 9b shows the conceptual configuration of a spring and radiation dashpot connected in parallel, followed by a plastic slider and viscous dashpot set in series. Unlike the Smith (1960) model, viscous and inertial effects of soils during driving are accounted for separately. The soil adjacent to the shaft is represented by a slider and viscous dashpot, expressed as

$$\tau = k_s w_s + c_s v_s \leq \tau_{limit} \quad (3)$$

$$k_s = G/D \quad (4)$$

$$c_s = \sqrt{G\rho_s} \quad (5)$$

Where:

G = Soil shear modulus
D = Pile diameter
v_s = Soil velocity
w_s = Soil movement
ρ_s = Soil mass density
τ_{limit} = Velocity-dependent limiting resistance at pile-soil interface when slip occurs, as represented by a viscous dashpot in parallel with plastic slider.

Equations 3 - 5 incorporate a power law formula for viscous enhancement of resistance under high velocity displacement, in accordance with the suggestions by Coyle and Gibson (1970)

$$\tau_{limit} = \tau_s[1 + \alpha(\frac{\Delta v}{v_{ref}})^{\beta}] \quad (6)$$

Where:

Δv = Relative velocity between pile segment and adjacent soil, normalised by v_{ref} (taken for convenience as 1.0 m/s)
α = Viscous parameter
β = Viscous parameter

Studies by Litkouhi and Poskitt (1980) led to taking β as 0.2-0.5 and α between 0.3 and 0.5 for sand, and up to 2 or 3 for clays (Randolph, 2003).

As suggested by Randolph and Simons (1986), pile and soil elements re-join when the shaft friction τ calculated from soil displacement and pile velocity falls below the assumed limiting interface equivalent static resistance, τ_s, as given below:

$$k_s w_s + c_s v_p \leq \tau_s \quad (7)$$

For end bearing, the 'continuum' base model developed by Deeks and Randolph (1995) adopts a broadly similar configuration to that for the shaft model, but accounts for two additional lumped masses.

$$K_b w_p + C_b v_p \leq q_b \quad (8)$$

$$K_b = \frac{4Gr_0}{1-v} \quad (9)$$

$$C_s = \frac{3.2r_o^2}{1-v}\frac{G}{V_s} = \frac{3.2r_o^2}{1-v}\sqrt{G\rho_s} \quad (10)$$

Where:

q_b = Static limiting base pressure
v = Poisson's ratio of soil beneath pile base
r_0 = Pile external radius

One advantage of the continuum model is possible simulation of the internal soil plug, with springs and dashpots similar to those representing the external soil.

The CAPWAP soil model makes no distinction between pile-soil interface and the far-field stiffness response. Both are captured together by a single elastic-perfectly plastic spring and viscous dashpot with an adjustment for the unloading stiffness. When using the radiation damping option, energy lost into the soil mass is included by considering a soil mass and dashpot as shown in Figure 9. The soil mass is by default taken as a cylinder 0.3m thick around the pile. This has been shown to give reasonable results with correlations on small diameter piles with capacities in the range 1 – 5MN (Likins et al, 1996).

2.11 Response comparison

A typical PAGE pile was selected for a detailed CAPWAP/IMPACT comparison (project A, location R). The pile length below the instruments was 78.5m and its penetration 65.5m. A control point set about 13m above the pile toe (1/5 of penetrated length) was selected for comparison of the soil model response.

At the pile top, a similar quality match was achieved (1.6 - 2.6 with CAPWAP, 1.2 with IMPACT) but with an interpreted pile resistance of 41 - 43MN with CAPWAP and about 50MN with IMPACT. Axial displacements at the control point in the two models are shown in Figure 10. While the final pile set is similar (pile set is one of the criteria for a signal match), the IMPACT model has a greater initial penetration and experiences a more significant rebound due to rebound of the far field soil.

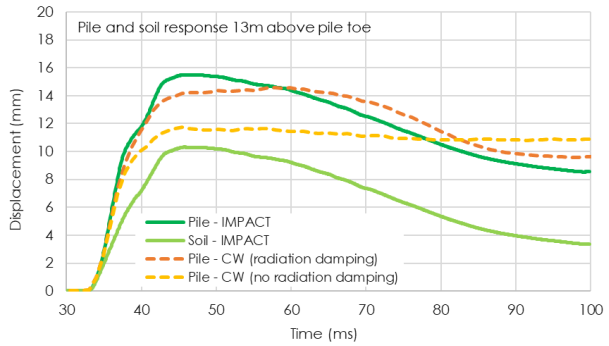

Fig. 10: Axial displacements.

Pile velocities in the two models are shown in Figure 11 along with the soil velocity of the IMPACT model.

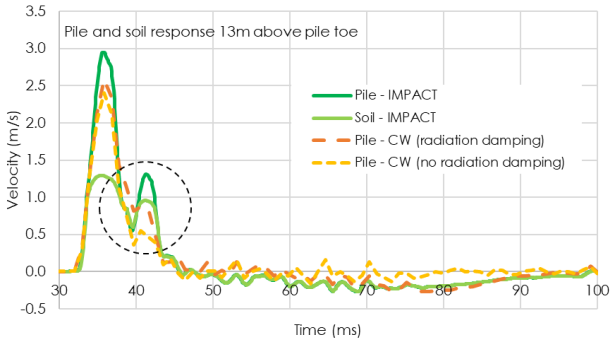

Fig. 11: Pile and soil velocity response.

Peak pile velocity in the IMPACT case is greater than in CAPWAP (less energy has been lost) but a significant difference occurs at about 42ms (shown circled) when the IMPACT pile velocity increases again following the toe reflection due to the softer IMPACT toe response. Additional penetration therefore occurs during the upward wave phase in IMPACT. Figure 12 shows a comparison of the upward travelling wave for the CAPWAP cases with and without radiation damping, and IMPACT. The upward travelling tension wave is strong in IMPACT, and less so with CAPWAP using radiation damping.

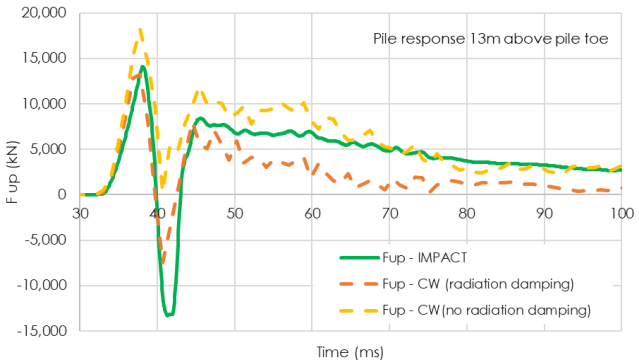

Figure 12: Upward traveling force wave

Further insights are gained into the shaft resistance soil models by investigating sub-elements of the model. Figure 13 shows the elements of the IMPACT soil response model without distinguishing whether they are active or not. The limiting "static" shear resistance of the interface is 107kPa, and the dynamic (static plus dynamic) resistance is referred to as the viscous (rate dependent) shear in Figure 13.

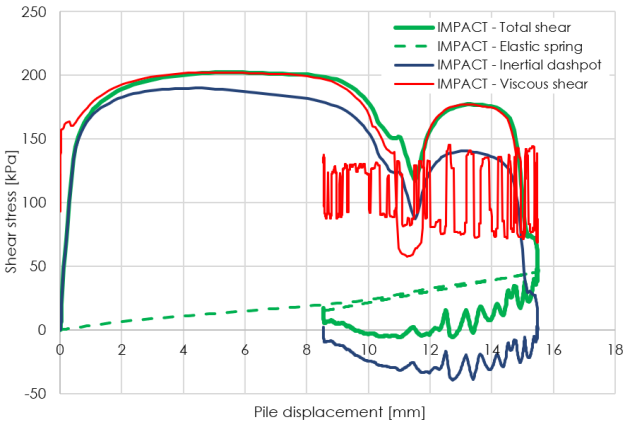

Fig. 13: Shear stress v pile displacement for IMPACT soil model.

The total shear resistance at the interface (solid green line) is controlled by the inertial soil dashpot in the early stages of loading until pile-soil slip occurs and the resistance is dominated by the high strain rate shearing resistance of the interface. This situation lasts until the pile "reattaches" to the soil as the upward travelling wave passes.

The two solutions are compared in Figure 14 (the CAPWAP model includes radiation damping). At the depth of the control point, CAPWAP indicates much higher total peak shearing resistance (due to higher viscous damping) over much of the penetration cycle but, as noted above, much lower during the upward travelling reflected wave due to the reduced velocities (Figure 14a).

Figure 14b shows the same data plotted against time, also showing the response of the soil plug in the IMPACT model (which was assigned internal shaft resistance only 10% of the external). The soil plug has little effect on the solution in this case. The IMPACT elastic spring (far field) gently rebounds following the peak loading. The soil response after the toe reflection differs significantly between the two models.

The higher total shear resistance indicated in the CAPWAP model results in a lower "static" pile resistance compared to IMPACT. This tendency is accentuated by the effect of the softer toe resistance in IMPACT and the additional downward movement of the pile as the tension wave moves up the pile but is mitigated by the greater elastic rebound of the far field soil spring.

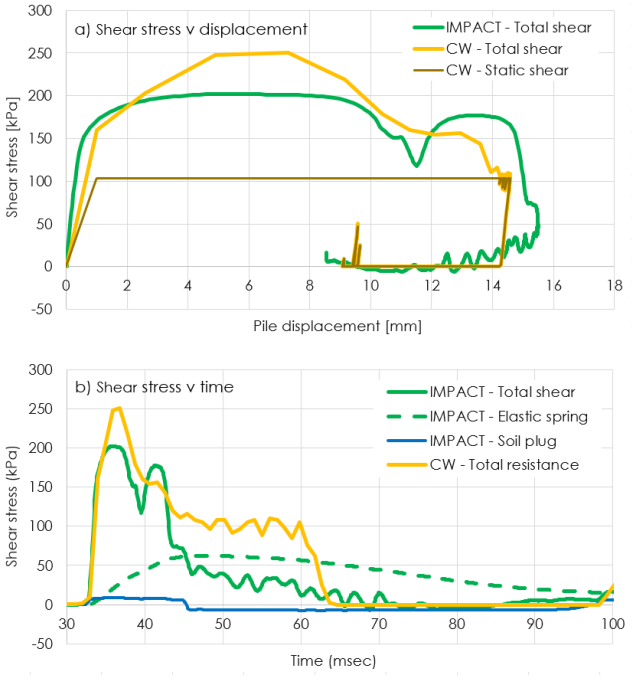

Fig. 14: Comparison of total shear stress

Considering the significant differences in local pile-soil response in the two models, PAGE's CAPWAP and IMPACT codes both delivered good signal matches, with reliable shaft resistance distributions and comparable overall setups. Therefore, their results were treated as being equally valid. However, it may be argued that IMPACT's continuum approach offers a more reliable theoretical approach for very large offshore piles, even though CAPWAP has a long history of successful application with smaller onshore piles.

3 ONSHORE/NEARSHORE STATIC AND DYNAMIC TEST CASE HISTORIES

3.1 General

Previous studies with relatively small piles (Likins et al, 1996 and Likins and Rausche, 2004) indicated good correlations between static resistances and those inferred from dynamic signal matching. However, it is possible that the correspondence between dynamic and static resistances varies with pile make up, scale, age, driving details and other factors. Further checking was required for PAGE. Noting that there are almost no published case histories in which concurrent dynamic and static tests were undertaken on separate open steel piles driven in sand, the PAGE team searched for new and independent datasets. As detailed below, three useful studies were identified involving steel piles with outside diameters up to 2m, driven in sand. Full site investigation and piling records were obtained from helpful colleagues in Germany, UK and Japan that allowed new, fully independent 'PAGE methodology' dynamic and static analyses to be undertaken.

3.2 Trans Tokyo Bay Highway

Shioi et al., (1992), Sawai et al., (1996) and Sawai (1998) describe nearshore static and dynamic testing on 1.6m and 2.0m OD piles driven for the 15km long Trans-Tokyo Bay (TTB) highway which connects Kawasaki and Kisarazu cities. Professors Shioi and Sakai kindly shared un-published data and answered several questions for the project. Strain gauges allowed shaft and base resistances to be separated. The PAGE team concentrated on:

- Dynamic data obtained with two 2.0m diameter 'ventilation tower' piles (T and R3) during driving and on restrike 43 hours later, as well as static compression and tension testing 52 days after driving. The primarily dense to very dense sands and silt/sands found over the maximum (30.6m) pile penetration depth were characterised by CPT and SPT profiling plus sampling.
- Dynamic tests on 1.6m diameter P8 bridge pier during driving and on restrike (76 hours later), as well as static compression tests 75 days after driving. SPT testing indicated dense sand and silt strata in approximately equal proportions over the 27m pile.

CAPWAP signal matching performed by the original contractors, and independently by PAGE, led to the 'ventilation tower' results summarised in Table 4 including the 52-day age static compression test. The PAGE EoID results for pile T fall between those derived by two teams (A and B) working on the TTB project. The dynamic and static results suggest that shaft setup increases from 1.33 (after 43 hours) to 2.89 after 52 days. These are accompanied by apparent increases in base resistance, although the latter may reflect shaft resistances that developed between the lowest strain gauge level and the lower pile tip and therefore be misleading. Cathie et al (2022) confirm Yang et al's (2017) and Lehane et al's (2017) assessment that the static pile test results fall close to predictions made with the ICP-05 CPT-based procedures and marginally above those made with the UWA-05 method.

Table 4: Interpreted resistance of TTB ventilation tower piles during driving and setup.

Pile	Condition/ Age	Analyst	Q_s (MN)	Q_{total} (MN)	Setup (shaft)
T	EoID	TTB-A	6.70	10.62	
T	EoID	TTB-B	10.15	15.09	
T	EoID	PAGE	8.75	11.18	
T-static	52 days	-	26.14	32.36	2.89
R3	EoID	TTB-A	13.67	19.14	
R3	BoR 43h	TTB-B	19.44	25.42	1.33

Notes:
Pile tip depth: T-30.6m, R3 – 26.1EoID, 26.6 BoR
Setup pile T from static resistance/PAGE EoD resistance

For the P8 piles, as with the ventilation tower piles, the PAGE team's analysis of the dynamic resistances was broadly comparable with those from TTB teams A and B. However, since the piles were fully instrumented with strain gauges and accelerometers mounted at 3m intervals along the shaft in the embedded section, these data were used by the PAGE team applying the multi-point method (MPM) – see Sawai et al, (1996) which was judged more

accurate than signal matching. The MPM method is a finite difference method using the force and acceleration data at the measuring points in the embedded section of the pile to determine the dynamic soil resistance and thus the static soil resistance (using the pile velocity).

The static compression load test performed after 75 days on one 1.6m OD pile at the P8 bridge pier site led to the results summarised in Table 5, which again indicated marked set up over the first weeks after driving.

The pile's axial load-depth distributions are plotted on Figure 15, showing the 75-day static test results (slightly smoothed around 19m) as well as the dynamic load distributions applying at EoID and on BoR 72 hours later, as interpreted by PAGE from strain gauges and accelerometers mounted along the pile shaft.

The load distributions from the dynamic and static tests show similar shapes, although the latter was clearly enhanced by ageing, with shaft setup factors around 1.5 (after 3 days) and 2.3 (after 75 days).

Table 5: Interpreted resistances of Pier P8 TTB pile during driving and after setup

Condition/ Age	Analyst	Q_s (MN)	Q_{total} (MN)	Setup (shaft)
EoID	PAGE	8.51	11.78	
BoR 76h	PAGE	13.03	15.17	1.53
Static 75 days	-	19.12	24.02	2.25

Note: BoR strike did not fully mobilise base resistance. Static toe capacity includes shaft resistance below lowest sensor (~1.7m).

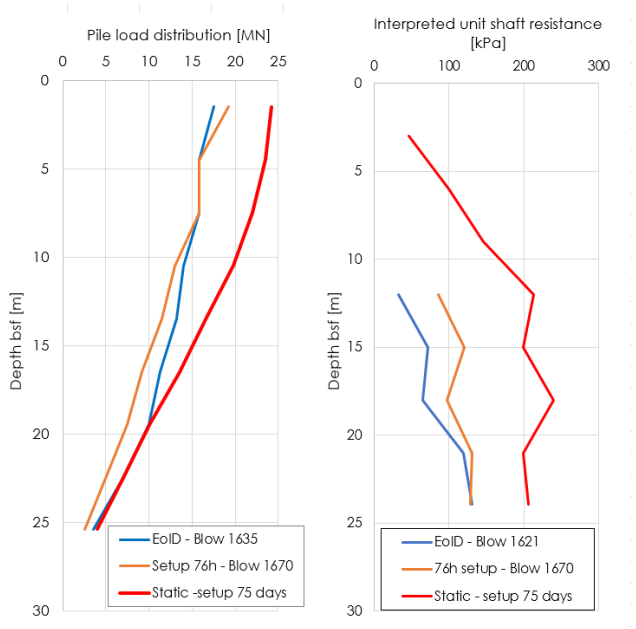

Fig. 15: Axial load distribution and interpreted unit shaft resistance for Trans Tokyo Bay pile tests on Pile P8.

3.3 EURIPIDES – Eemshaven, the Netherlands

The EURIPIDES (EURopean Initiative on PIles in DEnse Sands) joint industry project reported by Zuidberg and Vergobbi (1996), Fugro (2004) and Kolk et al. (2005) conducted comprehensive dynamic and static pile testing at Eemshaven port in the Netherlands on instrumented 763 mm OD driven steel open-tubular piles. CPT soundings and sampling indicate made ground to 5m, and low resistance Holocene fine sand to around 22m over mainly very dense, fine-to-medium Pleistocene sands with thin silt and clay layers that extend down to at least 50m depth.

Wen et al (2022) describe the first signal matching of the dynamic driving data, which was conducted for PAGE with both CAPWAP and IMPACT and enabled the first comparisons between dynamic and static compression tests. They analysed four cases and Figure 16 shows the full profile with depth of total soil resistance to driving (SRD), as predicted by three driveability approaches (Alm and Hamre 2001, and Stevens' method with upper and lower bound parameter sets) for driving to a 42.6m final penetration at the second test location. Also shown is the SRD trace back-analysed by Fugro (1996) from PDA measurements and the total SRDs predicted by PAGE for the final penetration depth, applying both CAPWAP and IMPACT to matching of signals recorded at EoID.

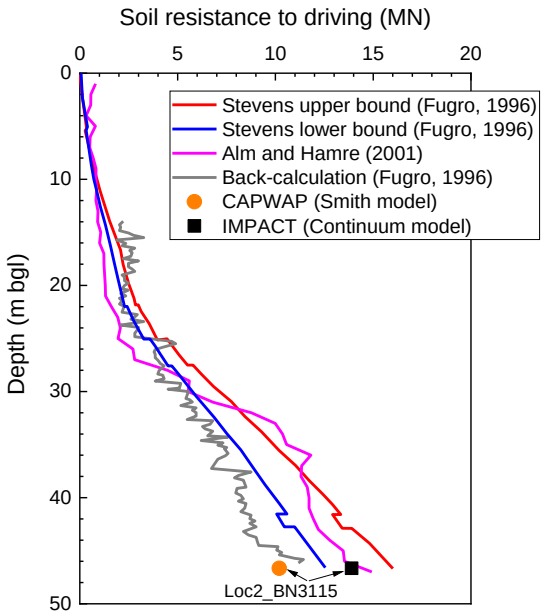

Fig. 16: Comparison between predicted and back-calculated soil resistance to driving: EURIPIDES, Location 2.

A static test proved a compressive resistance of 17.9MN 6 days after driving. A static re-test after 527 further days indicated capacity growth to at least 33.5MN. The shaft setup trends plotted in Figure 17 were assessed by comparing dynamic EoID and axial compression (ASC) tests covering the cases considered by the PAGE team.

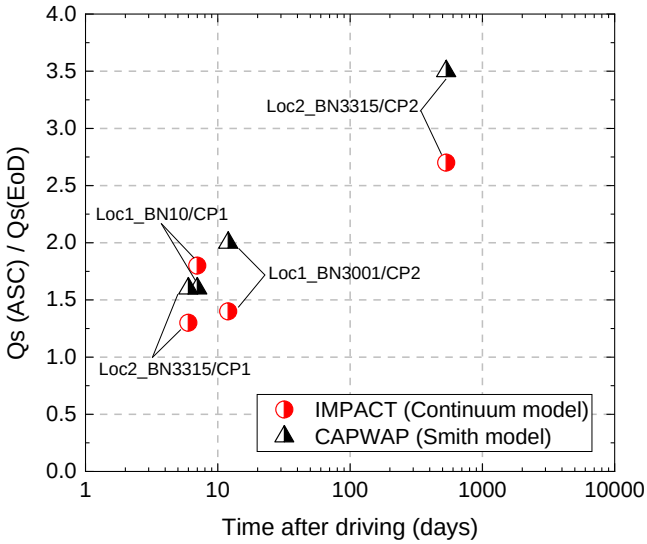

Fig. 17: Shaft setup Qs(ASC)/Qs(EoD) versus ageing days after driving from EURIPIDES pile tests.

The overall trends show shaft setup growing from 1.3 to 1.8 (over 6 to 12 days) and building to at least 2.7 after 533 days of ageing. Extrapolation back to a one-day age indicates Qs (ASC)/Qs (EoD) ≈1, implying comparable early age dynamic and static shaft resistances.

The PAGE study confirmed Jardine et al's (2005) conclusion that the ≈10-day age pile capacities match predictions made with the ICP-05 sand method closely. The 'static' driving shaft and tip SRDs correspond to around 63% and 53% respectively of the ICP-05 predictions.

3.4 Horstwalde

Bundesanstalt fur Materialforschung und prüfung (BAM) in 2012 conducted at Horstwalde, in Germany, dynamic, static and cyclic pile tests on 711mm OD (17.6m penetration) open-tubular steel piles driven in medium to very dense sands. The inland site was characterised by CPT and other profiling, Rücker et al., (2013). Further details were provided by BAM (2014) and their partner GuD; Figure 18 shows a general view of the testing arrangements.

The driving and re-strike monitoring data from tests on piles P1B and P4D were re-analysed for PAGE with CAPWAP and IMPACT, applying the team's standardised signal matching procedures.

The Horstwalde testing protocols included re-strikes after 13 and 39 days on P1B before its final test at a 546-day age, while P4D was re-struck at 10 days before a dynamic test at 30 days and a final static test in tension. Prior testing to failure is known to disrupt pile ageing in sand (Jardine et al 2006) and so the longer-term re-strikes provide lower bound estimates of the 'undisturbed' setup ratios. The PAGE analyses indicated similar total resistances by IMPACT and CAPWAP, although CAPWAP led to greater toe resistances. The shaft setup ratios shown listed in Table 6 are broadly comparable to those for TTB and EURIPIDES, despite the potential disruption of Hostwalde piles ageing by earlier re-strikes.

Fig. 18: General view of Horstwalde test site

The static tension test on P4D took place 4 days after its 30-day re-strike. The four blows applied caused 45mm further penetration, or 0.063D. Signal matching analyses indicated that shaft resistance reduced by ≈40% over the four blows. Allowing for this reduction and the 1.35 ratio between the compression and tension shaft resistances anticipated by ICP-05 calculations, the static resistance appears comparable to, although ≈15% below, that indicated by wave matching analysis of the final re-strike blow. The Horstwalde tests are compatible with the conclusion that signal matched dynamic tests shaft resistances are broadly equivalent to static test outcomes.

Table 6: Horstwalde setup factors assessed by PAGE IMPACT analyses

Case	Age at BoR (days)	Setup (total)	Setup (shaft)
P1B - BoR/ EoID	546	2.23	2.36
P4D - BoR/EoID	30	1.65	1.79

4 COMPILATION OF ONSHORE/NEARSHORE PILE AGEING DATA

The open driven steel pile sand case histories outcomes identified in Sections 1 and 3 are combined into a shaft setup-time scatter plot in Figure 19. The static and dynamic set-up trends appear broadly comparable and grow by 50% or more over the first ten days after driving. The older static tests indicate further increases with age, with set-up factors exceeding 2 after 100 days and perhaps 3 after 1000 days.

However, the Figure 19 dataset contains only two cases (both from TTB) that match offshore scales and conditions. As noted above, the TTB piles had unusual external driving shoes which could have affected their setup trends. The main emphasis in the PAGE study was therefore to rely primarily on offshore dynamic tests to identify how ageing progresses for large piles under marine conditions.

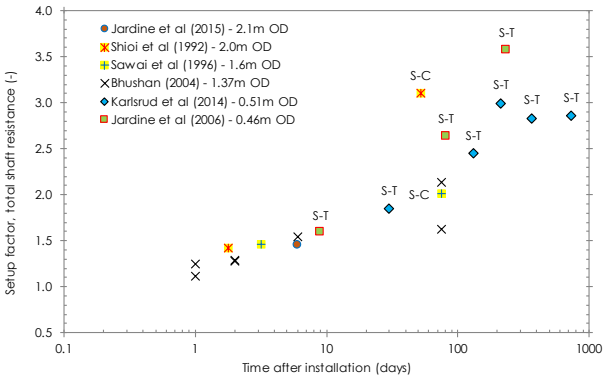

Note: S-T and S-C identifies cases in which setup was determined from static tension and compression tests, respectively, compared to EoID dynamic tests

Fig. 19: Shaft resistance setup trend, normalised by EoID, for piles with OD > 0.45m as reviewed in Section 1 and 3.

5 PAGE OFFSHORE DYNAMIC PILE TEST DATABASE

The PAGE offshore dynamic test database reported by Cathie et al (2022) covers 25 piles installed by hydraulic hammers with outside diameters (D) between 1.3m and 3.4m, length-to-diameter (L/D) between 8 and 53 and diameter-to-wall thickness (D/t) of 18 to 67.

Cathie et al (2022) note that the 11 cases with BoR tests conducted at ages greater than 50 days came from just 2 offshore projects. While their data points are considered reliable, further testing at greater ages at other sites would clearly be highly valuable in adding weight to the PAGE database and to the project's conclusions.

Most PAGE piles were driven in primarily medium dense to very dense North Sea sands, with variable silt contents, at nine separate sites. But the dataset includes a case offshore Indonesia, where significant layers of clay and gravel were present. However, the lower portion of the pile was embedded in a thick sand layer of sand which contributes a large proportion of overall shaft resistance. CPT data was available near all test piles; borehole sampling and description data were available for most. Soil/steel interface ring shear test results were available for 4 projects and the geotechnical data was sufficient to perform calculations for soil resistance during driving (Alm and Hamre, 2001) and ICP-05, Unified, UWA-05 and API static axial resistance calculations, following the methods' standard procedures.

Moderate-to-high quality dynamic EoID and BoR testing signals were available for all cases covering ageing (setup) periods between 8 hours and 374 days. Independent IMPACT signal matching analyses were undertaken for 12 piles. At ten locations the permanent pile displacements (sets) achieved on BoR fell below the 2.5mm accepted by PAGE as mobilising shaft resistance adequately. Alternative 'calibrated' wave equation analyses were undertaken with GRLWEAP to assess the Soil Resistance during Driving (EoD) for the 8 most valuable cases involving extended (52 to 81 day) ageing periods.

6 SETUP TRENDS FOR LARGE DIAMETER OFFSHORE PILES (PAGE DATA)

The following sections summarise the setup trends identified by the PAGE offshore study. The outcomes of signal matching (by CAPWAP and IMPACT) and adjusted wave equation analyses (by GRLWEAP) are summarised in terms of the setup ratio defined as:

Setup ratio = BoR resistance (R_{BoR})/ EoID resistance (R_{EoID})

The total (shaft plus base) resistance results are presented in Figure 20, with a hyperbolic curve of the form in Equation 11 with the fitting parameters summarised in Table 7.

$$y = A + B \tanh\left(C\ (t - 3)\right) \qquad (11)$$

Where:

y = parameter evaluated (setup or normalised resistance)

A = y-value 3 days after installation

B = maximum increase of y-value beyond 3 days (A+B defines y plateau)

C = parameter controlling the slope of the tanh function at 3 days

The fitted expression leads to a mean ratio of 1.0 between measured and predicted setup values, with a coefficient of variation equal to 0.09. Note that a setup factor plateau, of 1.78, appears to apply after around 30 days of ageing.

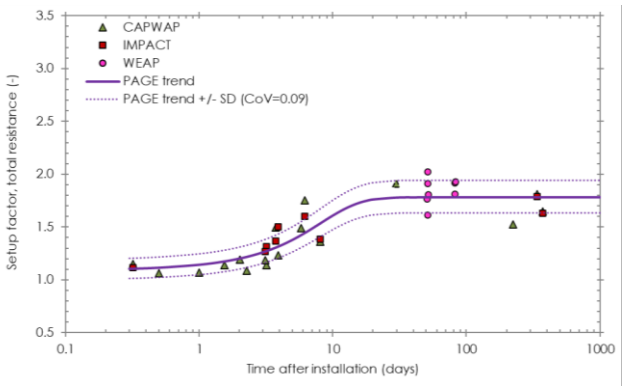

Fig. 20: Development of offshore PAGE piles' total resistance setup with time.

Table 7: PAGE tanh trends and Equation 11 fitting parameters.

Parameter evaluated	A	B	C	Fig.Ref.
Total resistance setup factor	1.26	0.520	0.1155	Fig. 19
Total shaft resistance setup factor	1.32	0.640	0.1174	Fig. 20

Figure 21 displays the corresponding plot for overall shaft resistance. The early BoR tests indicate only marginal shaft setup (around 1.1) within 12 hours of driving. Equation 11 (with the parameters in Table 7) gives an

average between the measured and predicted setup of 1.0 and a CoV = 0.08.

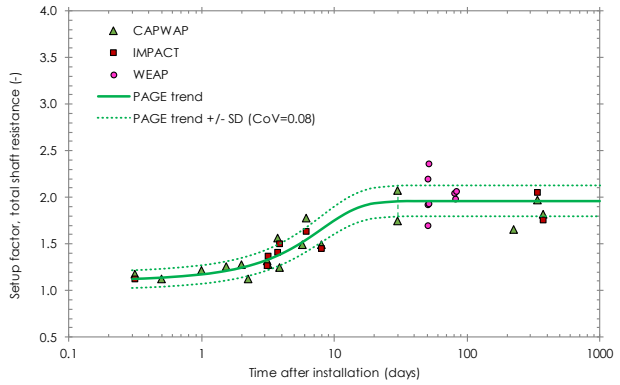

Fig. 21: Development of PAGE offshore piles' shaft resistances setup with time.

Plotting the early (<10-day) shaft setup data on a natural scale in Figure 22 shows that the rate of change is greatest within the first few days before declining after 3 to 4 weeks and reaching the average setup plateau of 1.96 after 30 days, as shown in Figure 21.

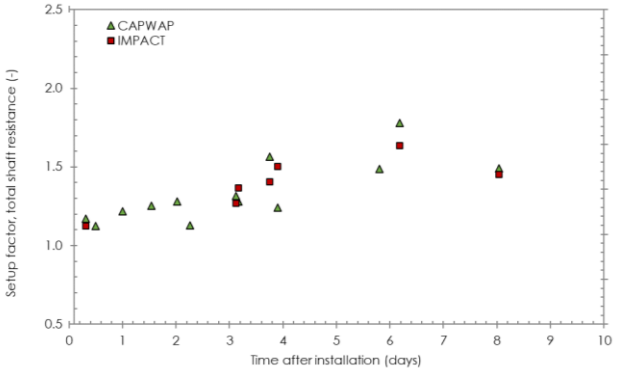

Fig. 22: Development of PAGE offshore piles' shaft resistance setup over first 10 days.

Toe resistance estimation through signal matching analyses is generally subject to greater uncertainty than applies to shaft analyses due to: i) potential residual axial stresses generated after each blow which are not explicitly simulated; ii) insufficient displacements to mobilise the pile's end bearing capacity during driving or restrike (Randolph, 2003; Salgado et al., 2015); iii) difficulties in resolving wave reflections arising from the pile annulus and the pile shaft close to the toe. Notwithstanding this caveat, PAGE signal matching revealed no clear set-up trends for toe resistance.

7 SETUP TRENDS FOR LARGE DIAMETER PILES (ALL DATA AVAILABLE)

The PAGE offshore shaft setup patterns are compared in Figure 23 with those derived in Section 1 to 3 from dynamic and static tests on mainly smaller, onshore and nearshore, piles. The comparison is clarified by plotting the offshore trend fitted with Equation 1 (± one CoV) and contrasting these with the scattered onshore/nearshore data points from Figure 19. Inspection shows:

- The offshore PAGE trends overlap with the onshore/nearshore dynamic and static patterns up to ages of around 30 days. However, their trends diverge at greater ages.
- The offshore piles' setup factor plateau (= 1.96) falls well below the average factor (≈2.9) obtained from static tension tests on smaller onshore or nearshore piles at ages greater than 50 days.
- Dynamic tests at >50 day ages on Bhushan (2004)'s 1.37m OD LAXT piles and the Horstwalde 0.71m OD piles indicated setup ratios closer to the PAGE offshore trend than most smaller piles.
- The Trans Tokyo Bay (TTB) tests on 2m diameter nearshore piles indicate more significant long term shaft setup than the PAGE trends. However, their setup ratios may be unrepresentative for piles of similar sizes driven offshore without the TTB piles' enlarged external shoes.

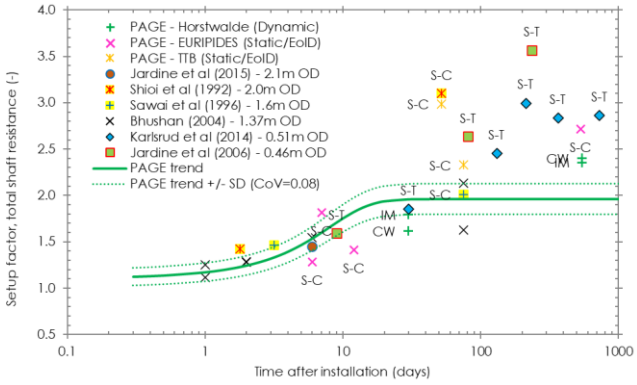

Notes: 1) S-T and S-C refer to setup based on EoD interpreted shaft resistance combined with tension or compression shaft resistance, respectively, from static tests after setup; 2) CW – CAPWAP, IM-IMPACT signal matching

Fig. 23: Development of shaft resistance setup with time: PAGE offshore data and other data summarised in Figure 19

The available evidence points to ageing having a different impact offshore to that seen with smaller onshore/nearshore piles. The differing shaft capacity growth trends could result from:

- Variations in the physio-chemical (or corrosion) reactions at play, which are affected by groundwater temperature, oxygen concentrations and salinity, or
- The different geometries, in particular the diameters and driving conditions.

8 NORMALISED PILE RESISTANCE FOR LARGE DIAMETER OFFSHORE PILES (PAGE DATA)

A key objective in assessing pile ageing is to investigate how the evolving static axial resistances relate to predictions from currently adopted pile design methods. Static axial resistance calculations were therefore undertaken for each case with modern CPT based methods as well as the API calculation method.

Plots are presented below to summarise the key findings by comparing PAGE's signal matching results for shaft resistance at EoID and BoR (R_m - measured), as normalised with static resistances determined with the Unified "full" method (R_c – calculated) and the ICP-05 method. The corresponding dynamic toe resistances all fall far below those mobilised under static compression testing. Different toe failure mechanisms apply under dynamic and static conditions; see Byrne et al (2012).

The shaft resistance ageing trends normalised by the Unified method analyses are shown in Figure 23, with an Equation 1 trend curve fitted with the parameters summarised in Table 9, while Figure 25 shows the corresponding curve normalised by ICP-05.

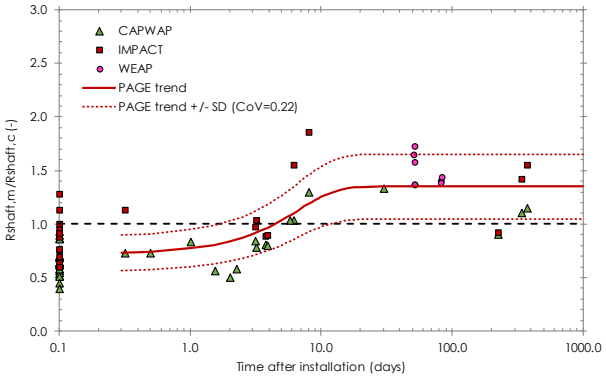

Fig. 24: PAGE offshore pile setup trends normalised by Unified total shaft resistance estimates

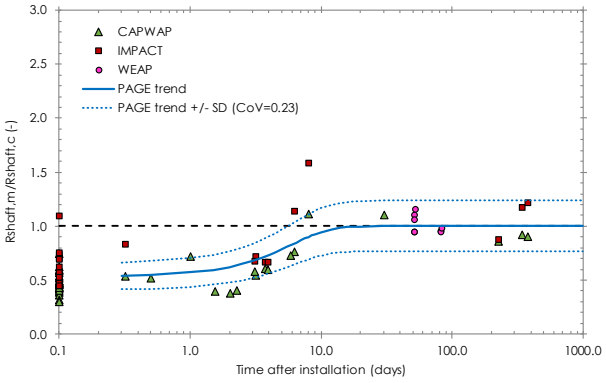

Fig. 25: PAGE offshore pile setup trends normalised by ICP total shaft resistance estimates.

The ratios of PAGE dynamic analysis resistances to the Unified method predictions rise from an average of 0.7 at EoID, reach unity at around 4 days and reach a plateau of 1.35 for BoR tests at ages exceeding 30 days. These trends imply a conservative bias for most practical applications.

When normalised by the ICP-05 method the PAGE dynamic analysis resistances rise from an average of 0.5 at EoID to reach an unexpectedly close mean of 1.0 on BoR for ages exceeding 30 days, indicating no long-term bias.

9 DIAMETER DEPENDENT SETUP TRENDS?

The contrasting offshore versus nearshore/onshore set-up trends summarised in Figure 23, suggest that the impact of ageing on shaft capacity may vary with pile diameter. To explore this further, Figure 26 plots the Unified normalised total shaft resistance for pile ages >20 days against pile diameter. Cathie et al (2022) present a similar assessment made with the ICP-05 method. While the information available does not allow any conclusive separation of how the various factors influence ageing in sand, a strong correlation emerges for the aged resistance, as normalized by the Unified method assessment to vary as:

$$R_{shaft,m}/R_{shaft,\ unified} = 1.13 + 0.65D_{ref}/D \quad (12)$$

Where D_{ref} = 1m is introduced to render the equation non-dimensional.

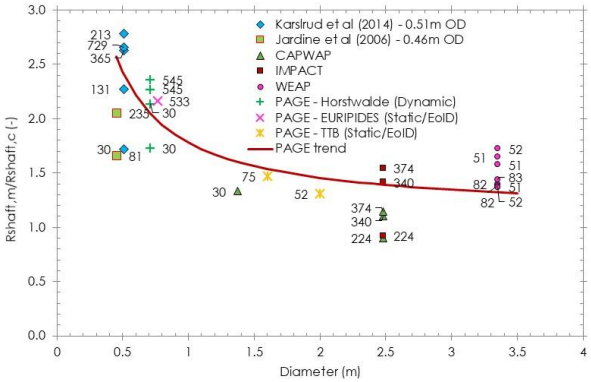

Notes: 1) PAGE data combined with other case histories, 2) Normalisation using Unified resistances, 3) Labels indicate number of days after driving when testing was performed (setup time)

Fig. 26: Dependence on pile diameter of total shaft capacities of all piles tested at ages greater than 20 days.

As indicated in the introduction, the ageing trends of piles with 0.4 to 0.5m diameters are similar to those of marginally smaller (down to 325mm OD) piles. However, micro-piles show less, although still very significant set up (Carroll et al 2020). So additional diameter-dependent processes appear to be influential at smaller scales and Equation 2 should not be applied when D<0.3m.

The PAGE study's findings have significant implications. However, it is important to recall the sparsity of the long-term data identified by the PAGE JIP covering large piles driven onshore, nearshore or offshore. Clearer trends may emerge from any new high-quality ageing tests on such piles. The trends indicated in this study may have been influenced by the polarised composition of the PAGE database, which combines mainly static tests on smaller-diameter onshore piles with larger-diameter offshore piles that were mostly tested dynamically. Offshore testing of long-term setup with small diameter piles by static means, or onshore dynamic testing of large diameter piles provide the best way of testing the PAGE conclusions.

The ageing trends seen over the first 20 days after driving do not vary systematically with pile diameter. Two potential (diameter independent) explanations for the approximate doubling in shaft capacity over this period are:

1) Possible roughening of the pile shaft through corrosion, or adherence of sand grains to the shaft leading to a diameter-independent increase in wall friction angle from critical state δ to critical state φ´. With typical sub-rounded to sub-angular silica media tested at modest effective stresses these angles may be estimated as 29º (possibly higher for finer sands) and 32º respectively. The ratio of their tangents is 1.13 (and possibly lower for fine sands), so this contribution is relatively modest.
2) Re-distribution of the effective stresses that develop during installation around the pile shaft. Jardine, (2020) reviews evidence from calibration chamber tests, advanced FE analyses (employing Arbitrary Lagrangian-Eulerian routines) and Discrete Element Modelling (DEM) that all point towards radial stresses being smaller on the shafts of displacement piles than in the sand mass, only a short distance from the shaft. Intense gradients are indicated that are made possible by even more extreme distributions of circumferential stresses. It is well known that such arching regimes can weaken over time due to creep and/or low-level cyclic loading and this could lead to radial stresses rising gradually on the pile shafts.

While analyses of open-ended pile installation currently present major challenges, it might be expected that the detailed outcomes might vary with D/t. Allowing for the separate influence of the interface friction angle gain discussed above, it appears plausible that the redistribution mechanism could provide most of the near doubling in capacities seen over the first 20-30 days.

The PAGE dataset also confirms that piles with diameters less than around 1m driven in onshore/nearshore environments develop more marked longer term capacity gains beyond 20 days that could not be detected in the limited set of long-term re-strikes on larger offshore piles. It appears that the longer-term normalised shaft resistance varies systematically with 1/D as shown in Figure 26. Potential explanations include both corrosion products building up and expanding the effective pile radius out into the soil mass and the associated increased pile roughness leading to greater dilation applying at the interface.

Cathie et al (2022) show that the marked long term capacity gains seen in the field with the 0.5 – 0.75m OD piles used at Dunkirk, Euripides and Larvik can be explained by relatively modest increases in interface dilation which would also explain the inverse relationship of shaft resistance with pile diameter as seen in Figure 26. Further checking is warranted, but their minor elaboration of existing design approaches provides a potentially robust and simple means of estimating long-term aged pile capacity for piles with diameters in the 0.3 to 3.5m range.

10 SUMMARY AND CONCLUSIONS

The PAGE JIP study collated 25 high-quality offshore cases for which resistances could be interpreted by dynamic analyses of end-of-initial driving (EoID) and beginning-of-restrike (BoR) blows after known setup periods. Strict quality assurance was applied to each case, ensuring that the necessary pile details were known, the dynamic data quality was sufficiently high, and the ground conditions were sufficiently well characterised to facilitate reliable dynamic analysis. Systematic, consistent, and rigorous numerical re-analysis was then applied to driving and re-strike blows to assess axial resistances that were compared with CPT-based pile capacity calculations, providing the first such database for large diameter offshore piles, for which no static pile test data is currently available.

PAGE's offshore pile analyses were complemented with both analysis of data from the literature and new analyses of two onshore, and one nearshore research case histories, where dynamic impact and static testing was conducted on comparable piles. The key conclusions reached are:

- Dynamic and static tests on open steel driven piles lead to broadly similar shaft capacities in sands, although dynamic base resistances fall far below static values and show no consistent tendency to manifest set-up.
- Open steel piles with outside diameters between 0.45m and 3.4m follow similar trends for shaft capacities to increase markedly in the days after driving in sand and approximately double within a month of installation.
- Offshore piles with diameters greater than 1m driven offshore appear to show little or no additional set up after 30 days, while smaller diameter onshore piles tested statically or dynamically show further marked capacity growth.
- Hyperbolic fitting equations have been proposed for the observed shaft setup trends.
- The interpreted long-term shaft capacities of large offshore piles match the ICP-05 CPT-based design predictions well but exceed the Unified CPT method by around 35%, suggesting a significant degree of conservatism.
- An inverse relationship with pile diameter has also been identified for the normalised long-term shaft resistances, covering the 0.3 to 3.5m pile diameter range.
- Potential explanations for the diameter dependency include corrosion product growth around the shaft and the variable impact of enhanced dilatancy that ageing induces at the pile-sand interface.
- Representative long-term capacity predictions may be made for the full range of pile diameters with ICP-05 by increasing the radial interface dilation term (Δr). Laboratory shear tests employing interfaces with CLA roughnesses $>d_{50}/10$ and appropriate normal stress levels can predict site-specific Δr values.
- The additional set-up caused by either enhanced dilation or corrosion product growth had a minimal effect on the large diameter PAGE offshore pile cases.

The PAGE outcomes improve understanding of driven pile ageing in sand and should aid future updating of the international practice and design recommendations

ACKNOWLEDGEMENTS

The Authors acknowledge gratefully the PAGE sponsorship by: BP, DEME Offshore, EnBW, Equinor, Jan de Nul, Scottish Power Renewables, Van Oord and Ørsted. They also thank the Project's Technical Review Panel members: Professor David White (University of Southampton), Dr Frank Rausche (Pile Dynamics Inc), Jens Bergan-Haavik (DNV GL, supported by Liv Hamre), Dr Neil Morgan (Lloyds Register) and Dr Oswald Klingmuller (GSP, supported by Dr Matthias Schallert). The project also benefitted from input provided by Dr Tingfa Liu and Mr Kai Wen at Imperial College London and from colleagues at Fugro (UK), BAM (Germany) and the Japanese Geotechnical Society who provided highly valuable additional unpublished data. Finally, we would like to acknowledge our Cathie colleagues Erdem Ozsu and Dr Chiara Prearo who performed much of the engineering work and CAPWAP signal matching, respectively.

REFERENCES

1) Alm, T., Hamre, L., 2001. Soil model for pile driveability predictions based on CPT interpretations. Presented at the International Conference On Soil Mechanics and Foundation Engineering.

2) API RP 2GEO, 2011. API RP 2GEO Geotechnical and Foundation Design Considerations.

3) Axelsson, G., 2000. Long-Term Set-Up of Driven Piles in Sand (No. TRITA-AMI PHD 1035 ISSN 1400-1284 ISRN KTH/AMI/PHD--1035--SE).

4) Baldi, G., Bellotti, R., Ghionna, V.N., Jamiolkowski, M., Lo Presti, D.C., 1989. Modulus of sands from CPTs and DMTs, in: Proc. XII ICSMFE, Rio de Janeiro. p. 170.

5) BAM, 2014. Experimenteller Tragfähigkeitsnachweis und Qualitätssicherung von Pfahlgründungen für Offshore Windkraftanlagen : Abschlussbericht zum Forschungsverbundprojekt. BAM Bundesanstalt für Materialforschung und -prüfung, Fachbereich 7.2, Ingenieurbau, Berlin. https://doi.org/10.2314/GBV:877878838

6) Bushan/Geofon (1997) Indicator pile driving report, Los Angeles Export Terminals (provided for PAGE project)

7) Bhushan, K, 2004. Design & installation of large diameter pipe piles for LAXT wharf, Conférence Contributions in Honor of George G. Gobel, ASCE, https://doi.org/10.1061/40743(142)21

8) Buckley, R.M., Kontoe, S., Jardine, R.J., Maron, M., Schroeder, F.C., Barbosa, P., 2017. Common pitfalls of pile driving resistance analysis - a case study of the Wikinger offshore wind farm, in: Proceedings of the 8th Int. Conf. on Offshore Site Investigation and Geotechnics. Presented at the Offshore site investigation and geotechnics - smarter solutions for future offshore developments, London, U.K.

9) Buckley, R.M., Jardine, R.J., Kontoe, S., Barbosa, P., Schroeder, F.C., 2020. Full-scale observations of dynamic and static axial responses of offshore piles driven in chalk and tills. Géotechnique 70, 657–681.

10) Byrne, T., Doherty, P., Gavin, K., Overy, R., others, 2012. Comparison of Pile Driveability Methods In North Sea Sand. Offshore Site Investig. Geotech. Integr. Technol.-Present Future.

11) Carroll, R., Carotenuto, P., Dano, C., Salama, I., Silva, M., Rimoy, S., Gavin, K., Jardine, R., 2020. Field experiments at three sites to investigate the effects of age on steel piles driven in sand. Géotechnique 70, 469–489. https://doi.org/10.1680/jgeot.17.P.185

12) Cathie, D., Jaeck, C., Ozsu, E., Raymackers, S., 2020. Insights into the driveability of large diameter piles. ISFOG.

13) Chow, F.C., 1997. Investigations into the behaviour of displacement pile for offshore foundations, PhD thesis, Imperial College London, UK.

14) Chow, F.C., Jardine, R.J., Brucy, F., Nauroy, J.F., 1998. Effects of time on capacity of pipe piles in dense marine sand. J. Geotech. Geoenvironmental Eng. 124, 254–264.

15) Coyle, H.M. and Gibson, G.C. (1970) Empirical damping constants for sands and clays, J. Soil Mech. Foundations, ASCE, Vol 96, SM3, 949-965.

16) Deeks, A.J., Randolph, M.F., 1995. A simple model for inelastic footing response to transient loading. Int. J. Numer. Anal. Methods Geomech. 19, 307–329. https://doi.org/10.1002/nag.1610190502

17) Fellenius, B. H. (1988). Variation of CAPWAP results as a function of the operator. Proc. of the 3rd Int. Conf. on the Application of Stress Wave Theory to Piles, Ottawa, Canada, pp. 814-825

18) Fugro Engineers B.V., 2004. Axial pile capacity design method for offshore driven piles in sand (Report to American Petroleum Institute No. P1003). Houston, TX, USA.

19) Gavin, K.G., Igoe, D.J.P., Kirwan, L., 2013. The effect of ageing on the axial capacity of piles in sand. Proc. ICE - Geotech. Eng. 166, 122–130.

20) Gavin, K., Jardine, R., Karlsrud, K., Lehane, B., 2015. The effects of pile ageing on the shaft capacity of offshore piles in sand, in: Frontiers in Offshore Geotechnics III. pp. 129–151.

21) Hannigan, P., Robinson, B., Dasenbrock, D., 2019. Wave Speeds in Large Diameter Open-End Steel Pipe Piles, in: Bullock, P., Verbeek, G., Paikowsky, S., Tara, D. (Eds.), 10th International Conference on Stress Wave Theory and Testing Methods for Deep Foundations. ASTM International, West Conshohocken, PA, pp. 394–406. https://doi.org/10.1520/STP161120170201

22) Jardine, R.J., Chow, F.C., 1996. New Design Methods for Offshore Piles. Marine Technology Directorate, London.

23) Jardine, R., Chow, F., Overy, R., Standing, J., 2005. ICP design methods for driven piles in sands and clays. Thomas Telford.

24) Jardine, R.J., Standing, J.R., Chow, F.C., 2006. Some observations of the effects of time on the capacity of piles driven in sand. Géotechnique 56, 227–244.

25) Jardine, R.J. (2013). Advanced laboratory testing in research and practice. 2nd Bishop Lecture. Proc. ICSMGE, Eds Delage et al., Presses des Ponts, Paris, Vol 1, pp. 35-55

26) Jardine, R., Thomsen, N., Mygind, M., Thilsted, C.L., 2015.

Axial capacity design practice for North European wind-turbine projects. Presented at the ISFOG.

27) Jardine, R.J., 2020. Geotechnics, energy and climate change: the 56th Rankine Lecture. Géotechnique 70, 3–59. https://doi.org/10.1680/jgeot.18.RL.001

28) Karlsrud, K., Jensen, T.G., Lied, E.K.W., Nowacki, F., 2014. Significant ageing effects for axially loaded piles in sand and clay verified by new field load tests, in: Offshore Technology Conference. Presented at the OTC, Offshore Technology Conference.

29) Kirsch, F., von Bargen, M., 2012. Offshore Windpark Nordsee Ost - Sichere Grundung bei Wind und Welle. Presented at the Baugrundtagung Mainz.

30) Kolk, H., Vergobbi, P., Baaijens, A., 2005. Results from axial load tests on pipe piles in very dense sands: the EURIPIDES JIP, in: Frontiers in Offshore Geotechnics: ISFOG 2005. 661-667.

31) Kuwano, R. (1999) The Stiffness and Yielding Anisotropy of Sand, PhD thesis, Imperial College London, UK.

32) Lehane, B.M., Schneider, J.A., Xu, X., 2005. The UWA-05 method for prediction of axial capacity of driven piles in sand, in: Frontiers in Offshore Geotechnics: ISFOG 2005. pp. 683–689.

33) Lehane, B. M., Li, Y., & Williams, R. (2013). Shaft capacity of displacement piles in clay using the cone penetration test. Journal of Geotechnical and Geoenvironmental Engineering, 139(2), 253-266

34) Lehane, B.M., Lim, J.K., Carotenuto, P., Nadim, F., Lacasse, S., Jardine, R., Van Dijk, B., 2017. Characteristics of Unified Databases for Driven Piles, in: OSIG 2017. Presented at the OSIG 2017, Society for Underwater Technology, London, UK, p. 162.

35) Lehane, B., Liu, Z., Bittar, E., Nadim, F., Lacasse, S., Jardine, R.J., Carotenuto, P., Jeanjean, P., Rattley, M., Gavin, K., Haavik, J., Morgan, N., 2020. A new “unified” CPT-based axial pile capacity design method for driven piles in sand, in: Proceedings of the 4th International Symposium on Frontiers in Offshore Geotechnics., American Society of Civil Engineers.

36) Likins, G, F.Rausche, G.Thendean and M.Svinkin, 1996. CAPWAP correlation studies, Proceedings of the Fifth International Conference on the Application of Stress-wave Theory to Piles, Orlando, FL, pp 447-464

37) Likins, G., Rausche, F., 2004. Correlation of CAPWAP with Static Load tests. Presented at the 7th Int. Conf. on the application of Stres-wave Theory on piles, Malaysia.

38) Lings, M.L., Dietz, M.S., 2005. The Peak Strength of Sand-Steel Interfaces and the Role of Dilation. Soils Found. 45, 1–14. https://doi.org/10.3208/sandf.45.1

39) Maynard, Alice.W., Hamre, L., Butterworth, D., Davison, F., 2019. Improved Pile Installation Predictions for Monopiles. ASTM - STP 1611-2019 - ASTM Stress Wave Theory Test. Methods Deep Found. 426. https://doi.org/10.1520/STP1611-EB

40) Novak, M., Nogami, T. and Aboul-Ella, F. (1978). Dynamic soil reactions for plane strain case. J.Eng. Mech. Div., ASCE, 104(EM4), 953-959;

41) Overy, R., 2007. The use of ICP design method for the foundations of nine platforms installed in the UK North Sea. Presented at the Offshore site investigation and geotechnics OSIG.

42) Parker, E. J., Jardine, R. J., Standing, J. R. & Xavier, J. (1999). Jet grouting to improve offshore pile capacity. Proceedings of the offshore technology conference, Houston, TX, USA, paper OTC 10828.

43) PDI, 2005. PDA-W Users Manual.

44) PDI, 2006. CAPWAP-Case pile wave analysis program.

45) PDI, 2010. GRLWEAP Background report.

46) PDI, 2014. CAPWAP Help.

47) Randolph, M.F., Simons, H.A., 1986. An improved soil model for one-dimensional pile driving analysis, in: 3rd International Conference on Numerical Methods in Offshore Piling. Presented at the 3rd International Conference on numerical methods in offshore piling, Editions Technip, Nantes, France, pp. 3–17.

48) Randolph, M.F., 2003. Science and empiricism in pile foundation design. Geotechnique 53, 847–875.

49) Randolph, M.F., 2008. IMPACT - Dynamic analysis of impact driving - User manual for version 4.2 (Feb 2003 release).

50) Rausche, F., Goble, G., Likins, G., 1985. Dynamic Determination of Pile Capacity. J. Geotech. Eng. 111. https://doi.org/10.1061/(ASCE)0733-9410(1985)111:3(367)

51) Rausche, F., Nagy,M.,Webster, S., and Liang, Liqun, 2009. CAPWAP and refined wave equation analyses for driveability predictions and capacity assessment of offshore pile installations, Proceedings 28th International Conference on Ocean, Offshore and Arctic Engineering, OMAE2009, ASME, pp1-9.

52) Rausche, F., Likins, G. & Liang, L. (2010). Static and dynamic models for CAPWAP signal matching. In Art of foundation engineering practice, pp. 534–553. West Palm Beach, FL, USA: American Society of Civil Engineers

53) Rimoy, S.P., 2013. Ageing and axial cyclic loading studies of displacement piles in sands (PhD Thesis). Imperial College London, London.

54) Rimoy, S., Silva, M., Jardine, R., Yang, Z.X., Zhu, B.T., Tsuha, C.H.C., 2015. Field and model investigations into the influence of age on axial capacity of displacement piles in silica sands. Géotechnique 65, 576–589.

55) Robertson P.K., 2016. Cone Penetration Test (CPT)-Based Soil Behaviour Type (SBT) Classification System—An Update. Canadian Geotechnical Journal, 53, 1910-1927.

56) Rücker, W., Karabeliov, K., Cuellar, P., Baeßler, M., Georgi, S., 2013. Großversuche an Rammpfählen zur Ermittlung der Tragfähigkeit unter zyklischer Belastung und Standzeit. Geotechnik 36, 77–89. https://doi.org/10.1002/gete.201200021

57) Simons, H. A. & Randolph, M. F. (1985). A new approach to one dimensional pile driving analysis. Proceedings of the 5th international conference on numerical methods in

geomechanics (eds T. Kawamoto and Y. Ichikawa), pp. 1457–1464. Nagoya, Japan: Balkema.

58) Salgado, R., Loukidis, D., Abou-Jaoude, G., Zhang, Y., 2015. The role of soil stiffness non-linearity in 1D pile driving simulations.

59) Sawai, 1996. Determination of the bearing capacity of large diameter pile from the dynamic loading test. 5th Int. Conf. Application of Stress-Wave Theory Piles 788–796.

60) Sawai, 1998. Dynamic measurement method of bearing capacity of large diameter steel pipe piles, PhD Dissertation (in Japanese).

61) Shibata. A, Kawabata, N, Wakiya, Y, Yoshizawa, Y, Hayashi, M. Matsumoto, T., 2000. A comparative study of static, dynamic and statnamic load tests of steel pipe piles driven in sand, Application of Stress-Wave Theory to Piles, Ed Niyama and Beim, Balkema, 583-590.

62) Shioi, Y., Yoshida, O., Meta, T., Homma, M., 1992. Estimation of bearing capacity of steel pipe pile by static loading and stress wave theory (Trans-Tokyo Bay Highway). Presented at the Application of stress-wave theory to piles, pp. 325–330.

63) Silva, M., 2014. Experimental study of ageing and axial cyclic loading effect on shaft friction along driven piles in sand. PhD thesis, University of Grenoble, Grenoble, France.

64) Skov, R., Denver, H., 1988. Time-dependence of bearing capacity of piles, in: Proc. Third International Conference on the Application of Stress-Wave Theory to Piles. Ottawa. pp. 25–27.

65) Svinkin, M. R., 2004. Some uncertainties in high-strain dynamic pile testing. Proc. Geo Trans 2004, Los Angeles, California, pp. 705-714

66) Yang, Z. x., Jardine, R. j., Zhu, B. t., Foray, P., Tsuha, C. h. c., 2010. Sand grain crushing and interface shearing during displacement pile installation in sand. Géotechnique 60, 469–482. https://doi.org/10.1680/geot.2010.60.6.469

67) Yang, Z.X., Guo, W.B., Jardine, R.J., Chow, F., 2017. Design method reliability assessment from an extended database of axial load tests on piles driven in sand. Can. Geotech. J. 54, 59–74. https://doi.org/10.1139/cgj-2015-0518

68) Zuidberg, H., Vergobbi, P., 1996. EURIPIDES, load tests on large driven piles in dense silica sands, in: Offshore Technology Conference.